Modelling, simulation and experimental verification of a wheeled-locomotion system based on omnidirectional wheels

Thesis submitted by:

B.Sc. Pedro Alonso Flores Alvarez

for the degree of
Master of Science in Mechanical Engineering

Supervising professors:

Pontificia Universidad Católica del Perú

Univ.-Prof. Dipl.-Ing.

Jorge Antonio Rodriguez Hernandez

Technische Universität Ilmenau

Univ.-Prof. Dr.-Ing. habil.

Klaus Zimmermann

Ilmenau-Germany

Statement

Hereby I declare, that I have elaborated the present work without any non-specified assistance. The people involved in the research, literature, as well as any other resource used in this thesis, has been completely specified throughout and at the end of the text.

1st March 2016, Ilmenau

……..
Signature

ABSTRACT

The following work focuses on the kinematic and dynamic study of a four-wheeled robot, which is equipped with omnidirectional Mecanum wheels. The main objective of the thesis is to obtain a mathematical model from which both the kinematics and kinetics of the robot can be analyzed. Furthermore, the study presents a methodology to optimize the torques (and subsequent associated voltages) provided by each of the motors on the robot for a given trajectory.

A system in which a non-powered trailer pulled by the robot is also analyzed at a kinematic level. In this stage, four different cases are considered. The construction of the trailer is also described on this work.

In the first chapter, the global state of the art on analysis and control of omnidirectional robots (with focus on robots with Mecanum wheels) is presented. In the second chapter, the physical considerations for the general movement of the robot are analyzed, in order to derive the kinematic constrain equations of the locomotion system. The differential equation of motion is then derived using Lagrange-equations with multipliers. This chapter presents as well the kinematic analysis for a robot-trailer system. The third chapter describes the general process on the design of the trailer, including the rejected ideas for its construction. The fourth chapter focuses on verifying the final results of the design process, as well as tests to check the mobility of the system. Conclusions and future work are analyzed on the final part of the document, as well as the references and the acknowledgments to all the people involved in the project.

TABLE OF CONTENTS

CHAPTER ONE

STATE OF THE ART

Development of mobile systems has acquired importance in the industry over the last years. One of the objectives which it pursuits is omnidirectional movement, which means that a vehicle can move in any direction while being on any orientation (Doroftei *et al.*, 2008). From the many methods that have been proposed to achieve such purpose, these can generally be classified as (1) methods based on conventional wheels and (2) methods based on special wheel designs (Tlale, 2006). In the first group, the presence of steering wheels in many designs (De Luca and Oriolo) gives the robot an omnidirectional (or almost omnidirectional) nature. Nevertheless, these systems require a considerable space for maneuvering, as their wheels are not allowed to move in the direction of their central axis.

In contrast, the second group focuses on sorting this restriction. In particular, Mecanum wheels do not have such constrain, allowing the design of systems in which their total velocity could point in any direction on the plane of motion. This characteristic also solves the issue of immediate maneuvering and zero-radius curves, a fact which makes such systems truly omnidirectional.

The original idea for the Mecanum wheels date as back as 1973, when engineer Bengt Ilon invented them during his time at the Swedish company Mecanum AB. The wheel design consists on a disc (which could also have an elliptical shape, such as in Ramirez-Serrano and Kuzyk) which has rollers attached at a certain angle with respect to the disc axis on its perimeter. The rollers are free to rotate along its own axis, but no slipping is allowed between them and the surface. The general idea is that, even though the main disc spins steadily around its own axis, the rollers provide a force that is not entirely perpendicular to such axis. An example on a modern Mecanum wheel design can be seen on figure 1.1.

Fig. 1.1. Mecanum wheel design from AndyMark.
Image taken from www.andymark.com

Even though until today the idea of Mecanum wheels remains the same, worldwide companies, especially the ones who deal with robotic systems, have developed several designs. Nevertheless, most of the wheels include rollers whose axes have either a $45°$ angle or are parallel to that of the central disc. The latter, however, are usually called omnidirectional wheels, rather than Mecanum ones.

Fig. 1.2. On the left, a Mecanum wheel. On the right, an omnidirectional wheel.
Both designs are property of VEX Robotics.
Image taken from www.vexrobotics.com

While the Mecanum wheel itself is not entirely omnidirectional, a robot that uses four wheels is. The movement is achieved by adding the combined effect of each wheel's rotational velocity on the system, which in the end produces a resultant force on the robot's center of gravity to produce motion. Several examples of translation and rotation of a four-Mecanum-wheeled system can be seen on figure 1.2.

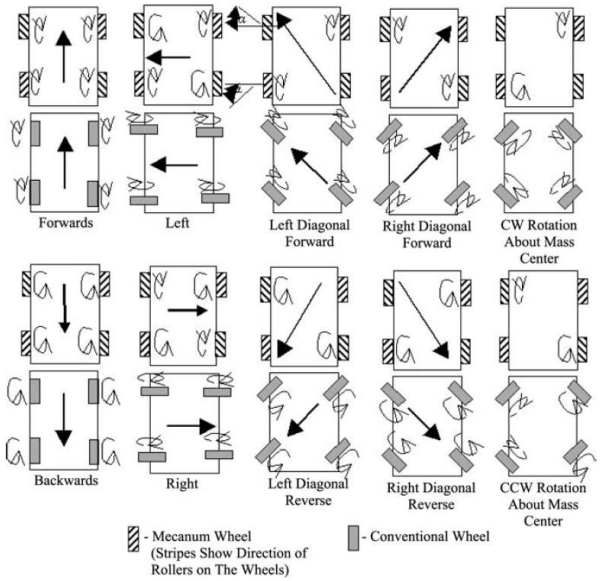

Fig 1.3. Different movement achieved by robot with Mecanum wheels and to the motion with conventional wheels.
Image taken from Tlale,2006.

As a result, the robot could achieve any trajectory (even non-continuous trajectories) by changing the speed on each of its wheels. This is especially useful for obstacle avoidance and movement optimization (the latter will be discussed briefly on a further chapter).

Not only have the design focused on planar motion, but also, robots like the one presented in Doroftei *et al.*, have considered that, even though this type of motion is most likely to occur during practical applications of this type of vehicles, small waves or perturbations on the ground could affect the control systems on the robot. This can cause problems while maneuvering it as the wheels could no longer rest on the ground. In the design by the author mentioned lines before, a suspension system is considered as part of the robot to overcome this problem.

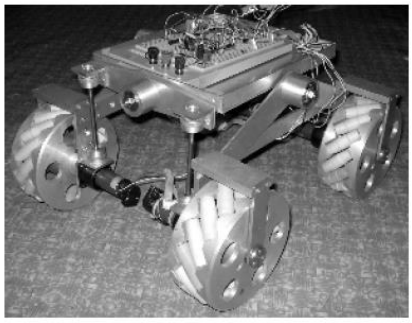

Fig 1.4. Robot prototype developed by Doroftei et al.
Image taken from "Design and control of an Omni-directional Mobile Robot"

Much interest has been shown in the way these robots are controlled, as they non-linear nature to achieve omnidirectional motion poses a challenge for both control systems and

robust actuator structures. Muir and Neuman discuss not only the kinematic approach to their robot *Uranus*, but also point out that, even though the actuators provide the right conditions for motion in three degrees of freedom, its structure is not robust, which could lead to actuator conflict. Just three of the four actuators are necessary to provide motion, leaving the fourth one dependent on the others. A solution is proposed by gearing to mechanically constrain the wheel motions so that all constrains are satisfied (Muir and Neuman, 1986).

Omnidirectional robots have found a vast application in the industry, as their motion capabilities are able to maneuver in small areas, such as factory aisles. Companies such as *Kuka Robotics* have developed several designs aimed for industry purposes, which for example, allow large machine elements or products to be transported around in an practical and safe way.

Fig. 1.5. Kuka's KMP omniMove, design for heavy-duty-transport. Image taken from www.kuka-robotics.com

The high maneuverability of these Mecanum robots can also make an impact on the mobility of disabled people. Abdelrahman uses a four-wheeled omnidirectional robot to improve a handicapped vehicle. It is mentioned that, even though theoretically all possible trajectories can be achieved with the robot, only simple "standard" trajectories can be achieved using a remote control, while a special software is required to control the driving moments applied to each wheel if trajectories that are more complex are to be achieved.

Kang *et al.* has also developed a prototype to aid disabled people in a factory environment. A robot with lifting and obstacle detection capabilities was developed in order to help limbed impaired workers on a factory to perform tasks such as working on a table, transporting elements and moving freely through the factory passages.

Fig. 1.6. Omnidirectional vehicle for disabled workers.
Image taken from Kang et al.

Another branch in which omnidirectional wheels seem to have had a big impact is on the development of the so-called Automated Guided Vehicle (AGV). Designs, such as the Robotnik's SUMMIT-X, allow automated omnidirectional movement both indoors and outdoors, thanks to its four Mecanum wheels, each one powered by one independent motor.

Fig. 1.5. SUMMIT-X from Robotnik for automated omnidirectional motion.
Image taken from www.robotnik.eu

The kinematics of these robots can be solved in different ways. Authors like Yunan *et al.*

Even though robots can be used individually to perform tasks, sometimes it is necessary to use articulate several vehicles, assembling the so-called robot-trailer systems. The kinematic constrains on these systems makes them in many cases, in the light of control engineering, highly nonlinear and underactuated, which naturally implies that their maneuverability has a high level of difficulty (Martínez *et al.* 2008).

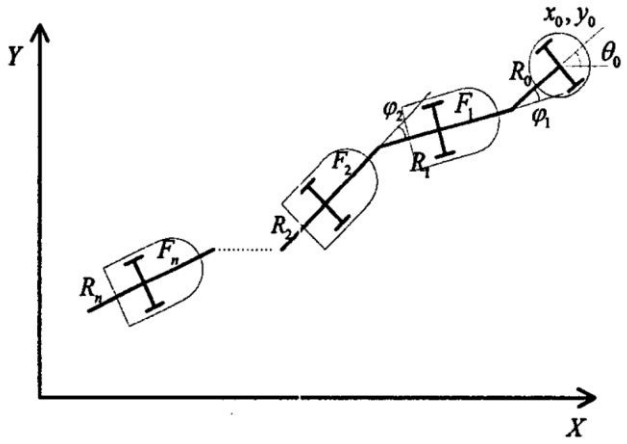

Fig. 1.6. Robot and passive trailers system.
Image taken from Park et al.*, 2004*

Most of the time, the driving part of the system is assumed by a non-omnidirectional robot, such as the one analyzed by De Luca and Oriolo. In their study, a steering-wheeled robot is assumed the driving part of the system, as well as their trailers being attached to each other's axles midpoints (a condition called *zero hooking*).

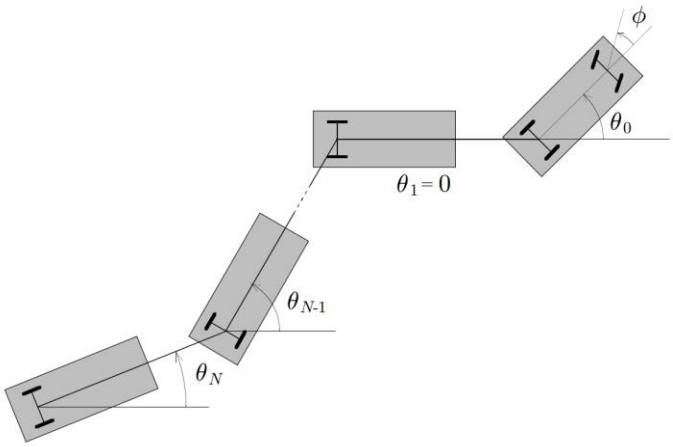

Fig. 1.7. Robot-trailer system analyzed by De Luca and Oriolo.
Image taken from De Luca and Oriolo.

Control of these systems can be even more challenging that the one of a non-holonomic robot itself. Park *et al.* suggested a method for the backward motion in which, if the trajectory of the *n*'th trailer is controlled, the trajectory of all the other trailers can be eventually controlled, even that of the driving robot. The method was further verified using a real robot-trailer system, which was to follow a linear and a circular path.

The starting point for the development of an omnidirectional robot is the kinematic analysis. This can be solved from two approaches. Authors like Yunan *et al.*, Kim *et al.* and

one of the kinematic models from Abdelrahman develop an approximate approach using a pseudo-inverse matrix (least squares method) to solve the kinematics equations for the robot. In the following chapter, the full kinematics and dynamics of a general Mecanum-wheeled robot will be analyzed to present an exact solution to the equations of motion for an omnidirectional robot with Mecanum wheels.

CHAPTER TWO

KINEMATICS AND DYNAMICS OF A ROBOT WITH FOUR MECANUM WHEELS AND A ROBOT- TRAILER SYSTEM

2.1. Analysis of One Wheel

The main objective of analyzing one wheel is to derive the constraint equation involved in the no-slip condition given to the roller. Given the following scheme:

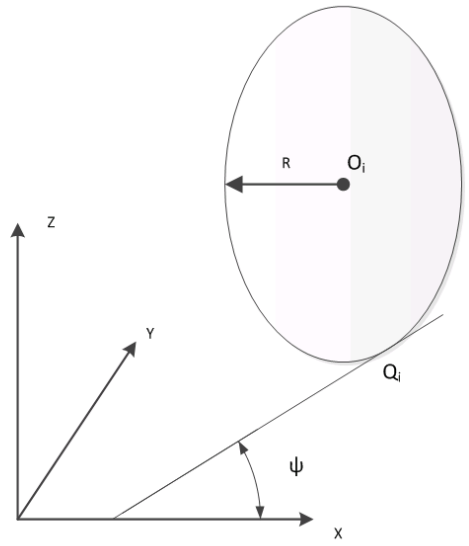

Fig. 2.1. Schematic drawing of a Mecanum wheel with an angle ψ in the XY plane

The point Q_i in Fig. 1 represents the center of the roller in contact with the ground at any time. Analyzing the velocity vectors in the XY plane will give the constraint equations needed

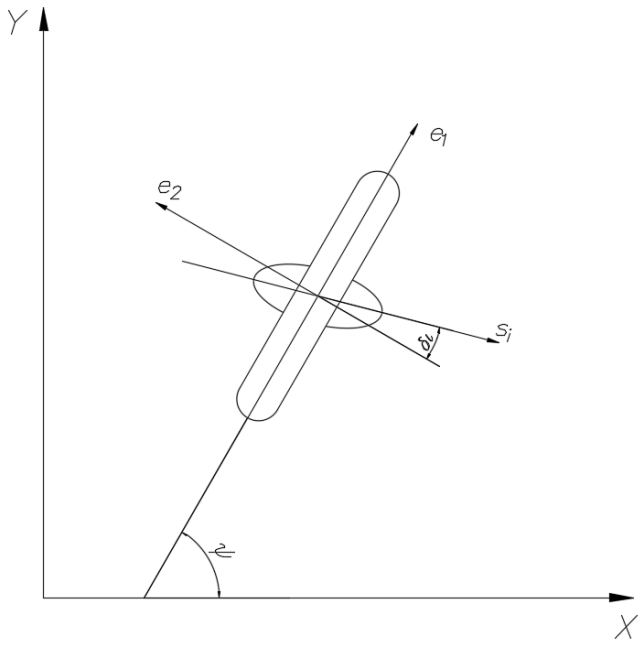

Fig. 2.2. Analysis of the wheel and the roller in the XY plane

The main constraint is the fact that the velocity of the point Q_i has no component over the unit vector $\overrightarrow{s_i}$, which follows the axis of the roller. This guarantees the no-slip condition of the wheel in a direction along the mentioned axis.

The unit vector $\overrightarrow{s_i}$ can be described in terms of a pair of axis $(\overrightarrow{e_1}, \overrightarrow{e_2})$ .The first one has an angle ψ with the horizontal X axis; the second one, is perpendicular to the first one following the right-thumb rule. It can be observed that the vector $\overrightarrow{s_i}$ has an angle δ_i measured from the axis $\overrightarrow{e_2}$. Thus:

$$\overrightarrow{s_i} = \sin(\delta_i)\,\overrightarrow{e_1} - \cos(\delta_i)\overrightarrow{e_2}$$

Both vectors $(\overrightarrow{e_1}, \overrightarrow{e_2})$ can be also written by their components in the XY plane:

$$\overrightarrow{e_1} = (\cos(\psi)\,, \sin(\psi))$$

$$\overrightarrow{e_2} = (-\sin(\psi)\,, \cos(\psi))$$

Then, rewriting the vector $\overrightarrow{s_i}$ results in:

$$\overrightarrow{s_i} = (\sin(\psi + \delta_i)\,, -\cos(\psi + \delta_i))$$

Applying the no-slip condition in the direction of $\overrightarrow{s_i}$ of the point Q_i:

$$\overrightarrow{v_{Q_i}} \cdot \overrightarrow{s_i} = 0$$

$$(\dot{x}_{Q_i}, \dot{y}_{Q_i}) \cdot (\sin(\psi + \delta_i), -\cos(\psi + \delta_i)) = 0$$

It is convenient to write the velocity of point Q_i in terms of the velocity of the center O_i of the wheel, for further analysis purposes. For this analysis, it will be considered that the wheel can turn around its axis with an angular velocity $\dot{\varphi}_i$. Using rigid dynamics kinematics:

$$\overrightarrow{v_{Q_i}} = \overrightarrow{v_{O_i}} + \overrightarrow{\omega_i} \times \overrightarrow{O_i Q_i}$$

$$(\dot{x}_{Q_i}, \dot{y}_{Q_i}) = (\dot{x}_{O_i}, \dot{y}_{O_i}) + (\dot{\varphi}_i \overrightarrow{e_2} + \dot{\psi}\overrightarrow{e_z}) \times (-R\overrightarrow{e_z})$$

$$(\dot{x}_{Q_i}, \dot{y}_{Q_i}) = (\dot{x}_{O_i}, \dot{y}_{O_i}) - R\dot{\varphi}_i(\cos(\psi), \sin(\psi))$$

Therefore:

$$\dot{x}_{Q_i} = \dot{x}_{O_i} - R\dot{\varphi}_i \cos(\psi)$$

$$\dot{y}_{Q_i} = \dot{y}_{O_i} - R\dot{\varphi}_i \sin(\psi)$$

Replacing these values in the constraint equation and operating:

$$\dot{x}_{O_i} \sin(\psi + \delta_i) - \dot{y}_{O_i} \cos(\psi + \delta_i) - R\dot{\varphi}_i \sin(\delta_i) = 0$$

Which is the constraint equation for a Mecanum wheel with no-slip condition along the axis of its roller.

2.2. Analysis of a four-wheeled Robot using Mecanum wheels

The last analysis was made in order to derive the constraint equation for one Mecanum wheel in a random position in terms of the velocity of its center. This will be used to write the velocity of each wheel in terms of its position with respect to the center of gravity of the robot.

For this purpose, fig. 3 shows the general dimensions of the robot, considering a random location of its center of gravity.

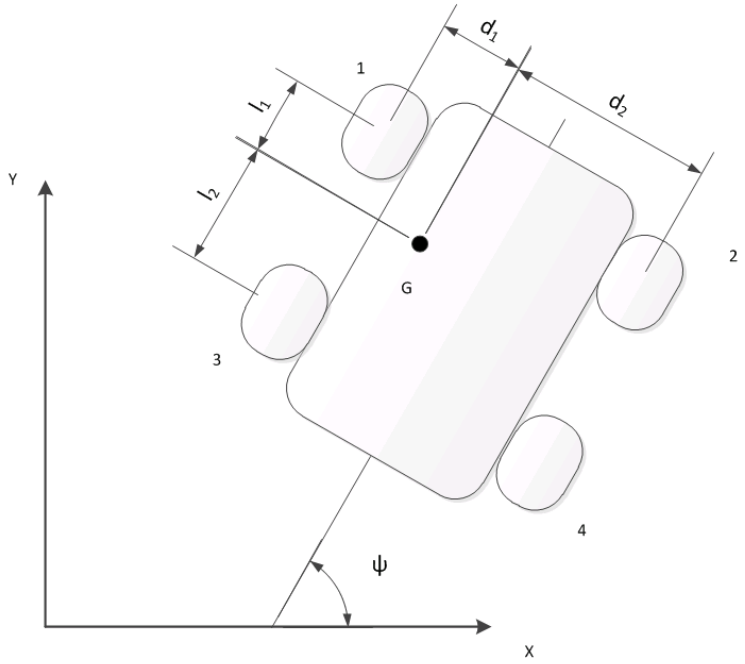

Fig. 2.3. Four wheeled robot with asymmetric center of gravity G

To derive the velocities of the center x_{O_i} of the wheels, the location of these must be found:

$$x_{O_1} = x_G + l_1 \cos(\psi) - d_1 \sin(\psi)$$

$$y_{O_1} = y_G + l_1 \sin(\psi) + d_1 \cos(\psi)$$

$$x_{O_2} = x_G + l_1 \cos(\psi) + d_2 \sin(\psi)$$

$$y_{O_2} = y_G + l_1 \sin(\psi) - d_2 \cos(\psi)$$

$$x_{O_3} = x_G - l_2 \cos(\psi) - d_1 \sin(\psi)$$

$$y_{O_3} = y_G - l_2 \sin(\psi) + d_1 \cos(\psi)$$

$$x_{O_4} = x_G - l_2 \cos(\psi) + d_2 \sin(\psi)$$

$$y_{O_4} = y_G - l_2 \sin(\psi) - d_2 \cos(\psi)$$

From these equations, the velocities can be calculated:

$$\dot{x_{O_1}} = \dot{x_G} - l_1\dot{\psi}\sin(\psi) - d_1\dot{\psi}\cos(\psi)$$

$$\dot{y_{O_1}} = \dot{y_G} + l_1\dot{\psi}\cos(\psi) - d_1\dot{\psi}\sin(\psi)$$

$$\dot{x_{O_2}} = \dot{x_G} - l_1\dot{\psi}\sin(\psi) + d_2\dot{\psi}\cos(\psi)$$

$$\dot{y_{O_2}} = \dot{y_G} + l_1\dot{\psi}\cos(\psi) + d_2\dot{\psi}\sin(\psi)$$

$$\dot{x_{O_3}} = \dot{x_G} + l_2\dot{\psi}\sin(\psi) - d_1\dot{\psi}\cos(\psi)$$

$$\dot{y_{O_3}} = \dot{y_G} - l_2\dot{\psi}\cos(\psi) - d_1\dot{\psi}\sin(\psi)$$

$$\dot{x_{O_4}} = \dot{x_G} + l_2\dot{\psi}\sin(\psi) + d_2\dot{\psi}\cos(\psi)$$

$$\dot{y_{O_4}} = \dot{y_G} - l_2\dot{\psi}\cos(\psi) + d_2\dot{\psi}\sin(\psi)$$

If these equations are replaced with the general equation of constraint for each wheel, the following system of constraint equations is achieved:

$$\dot{x_G}\sin(\psi + \delta_1) - \dot{y_G}\cos(\psi + \delta_1) - l_1\dot{\psi}\cos(\delta_1) - d_1\dot{\psi}\sin(\delta_1) - R\dot{\varphi_1}\sin(\delta_1) = 0$$

$$\dot{x_G}\sin(\psi + \delta_2) - \dot{y_G}\cos(\psi + \delta_2) - l_1\dot{\psi}\cos(\delta_2) + d_2\dot{\psi}\sin(\delta_2) - R\dot{\varphi_2}\sin(\delta_2) = 0$$

$$\dot{x_G}\sin(\psi + \delta_3) - \dot{y_G}\cos(\psi + \delta_3) + l_2\dot{\psi}\cos(\delta_3) - d_1\dot{\psi}\sin(\delta_3) - R\dot{\varphi_3}\sin(\delta_3) = 0$$

$$\dot{x_G}\sin(\psi + \delta_4) - \dot{y_G}\cos(\psi + \delta_4) + l_2\dot{\psi}\cos(\delta_4) + d_2\dot{\psi}\sin(\delta_4) - R\dot{\varphi_4}\sin(\delta_4) = 0$$

As there are four constraint equations (one for each wheel), and seven unknowns, the system has three degrees of freedom. Thus, three independent variables are required as data to solve the system.

The constraint equations can be written in matrix form, with the angular velocities of the wheels as unknowns. This system can be considered the inversed kinematics system of equations, where for a given velocity of the center of mass G and a specific general angular velocity $\dot{\psi}$, the required angular velocities of the wheels can be calculated.

$$\begin{bmatrix} \sin(\psi+\delta_1) & -\cos(\psi+\delta_1) & -l_1\cos(\delta_1)-d_1\sin(\delta_1) \\ \sin(\psi+\delta_2) & -\cos(\psi+\delta_2) & -l_1\cos(\delta_2)+d_2\sin(\delta_2) \\ \sin(\psi+\delta_3) & -\cos(\psi+\delta_3) & l_2\cos(\delta_3)-d_1\sin(\delta_3) \\ \sin(\psi+\delta_4) & -\cos(\psi+\delta_4) & l_2\cos(\delta_4)+d_2\sin(\delta_4) \end{bmatrix} \begin{bmatrix} \dot{x_G} \\ \dot{y_G} \\ \dot{\psi} \end{bmatrix} = \begin{bmatrix} R\dot{\varphi_1}\sin(\delta_1) \\ R\dot{\varphi_2}\sin(\delta_2) \\ R\dot{\varphi_3}\sin(\delta_3) \\ R\dot{\varphi_4}\sin(\delta_4) \end{bmatrix}$$

Likewise, three angular velocities $\dot{\varphi_1}$, $\dot{\varphi_2}$ and $\dot{\varphi_3}$ can be given, resulting in the following system of equations:

$$\begin{bmatrix} \sin(\psi+\delta_1) & -\cos(\psi+\delta_1) & -l_1\cos(\delta_1)-d_1\sin(\delta_1) & 0 \\ \sin(\psi+\delta_2) & -\cos(\psi+\delta_2) & -l_1\cos(\delta_2)+d_2\sin(\delta_2) & 0 \\ \sin(\psi+\delta_3) & -\cos(\psi+\delta_3) & l_2\cos(\delta_3)-d_1\sin(\delta_3) & 0 \\ \sin(\psi+\delta_4) & -\cos(\psi+\delta_4) & l_2\cos(\delta_4)+d_2\sin(\delta_4) & -R\sin(\delta_4) \end{bmatrix} \begin{bmatrix} \dot{x_G} \\ \dot{y_G} \\ \dot{\psi} \\ \dot{\varphi_4} \end{bmatrix} = \begin{bmatrix} R\dot{\varphi_1}\sin(\delta_1) \\ R\dot{\varphi_2}\sin(\delta_2) \\ R\dot{\varphi_3}\sin(\delta_3) \\ 0 \end{bmatrix}$$

Nevertheless, as the velocity of the center of mass depends on ψ, the system cannot, in general, be solved by direct integration (non-holonomic) and thus, must be solved numerically.

As it can be observed, functions of time for the angular velocities of the first three wheels can be used as inputs, resulting in different trajectories for the center of mass of the robot.

To simulate the results, the following parameters were considered:

$$l_1 = 100\ mm, l_2 = 100\ mm, d_1 = 50\ mm, d_2 = 50\ mm, \delta_1 = \delta_4 = 45°,$$

$$\delta_2 = \delta_3 = -45°, R = 10\ mm$$

Also, a number of 50 iterations were used to solve the system. The following results were achieved by varying the angular velocities of the wheels. In all cases, the trajectory of the center of mass is shown in Fig. 4.

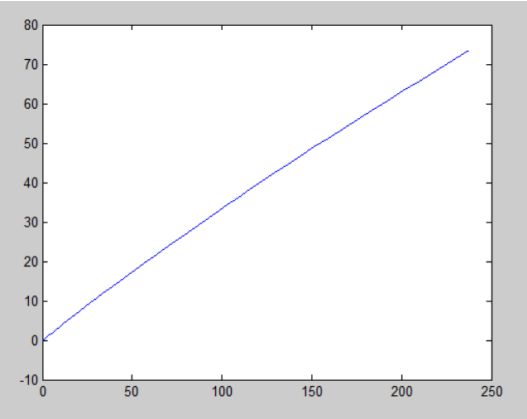

Fig.2.4. Trajectory obtained with $\dot{\varphi}_1 = 0$ and $\dot{\varphi}_2 = \dot{\varphi}_3 = t$

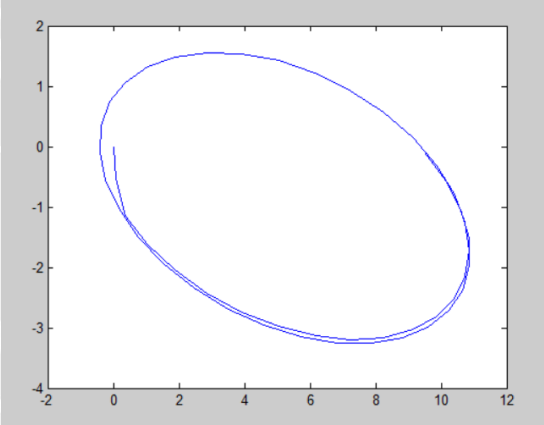

Fig.2.5. Trajectory obtained with $\dot{\varphi}_1 = 0$, $\dot{\varphi}_2 = \sin(t)$, $\dot{\varphi}_3 = \cos(t)$

The inverse kinematics equations can also be solved using Runge-Kutta methods, in order to obtain the functions $\varphi_1(t), \varphi_2(t), \varphi_3(t)$ and $\varphi_4(t)$. These functions are then utilized to follow a determined trajectory of the center of mass with a determined angular velocity.

The advantage of solving the inverse kinematics equations is that, for a given trajectory, the required functions $\varphi_i(t)$ can be calculated numerically. Several examples for different trajectories are illustrated in the following figures:

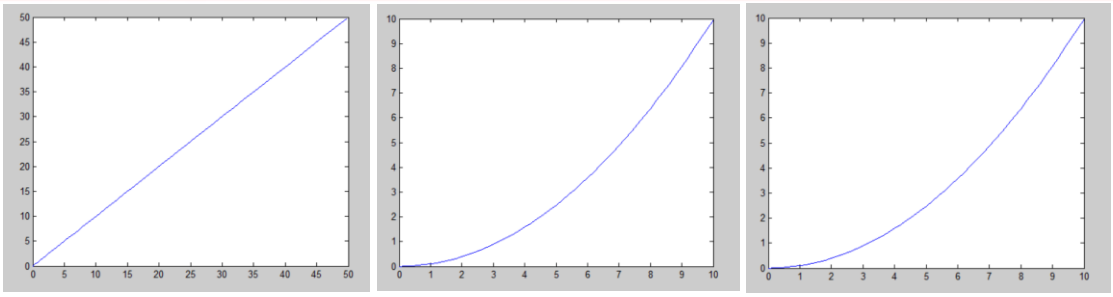

Fig.2.6. From left to right: Trajectory of the center of mass, resultant function for φ_2 and φ_3.

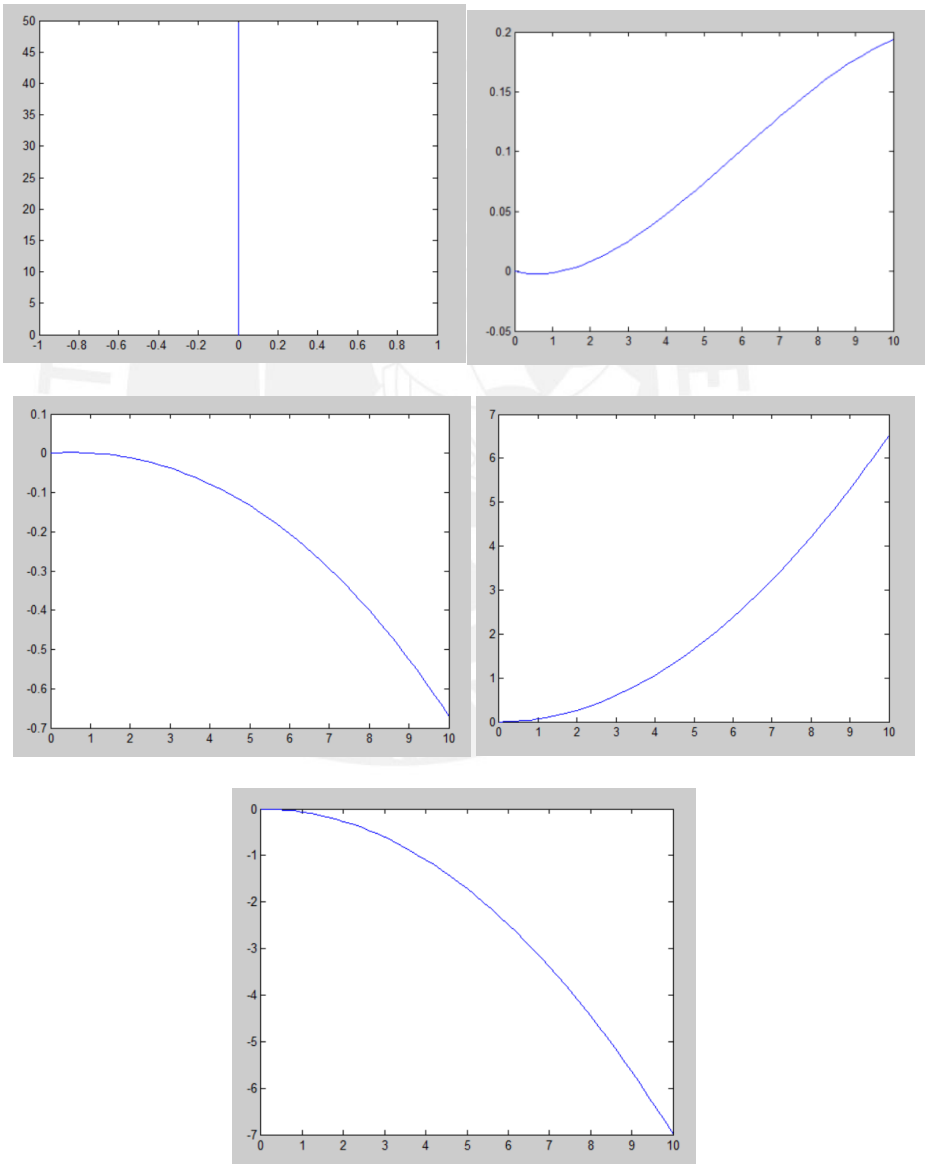

Fig.2.7. From left to right, top to bottom: Trajectory of the center of mass, resultant function for φ_1, φ_2 , φ_3 and φ_4.

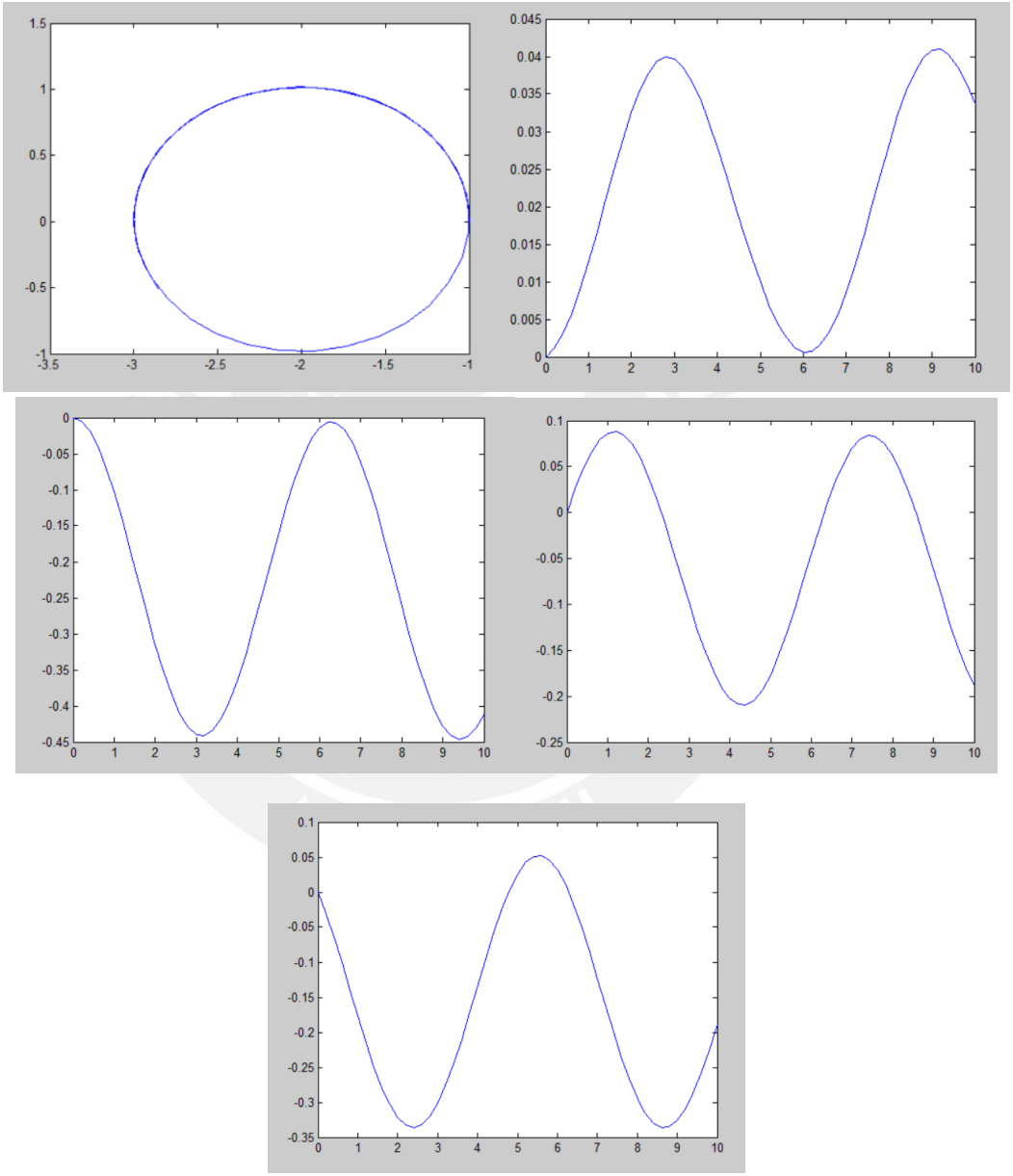

Fig.2.8. From left to right, top to bottom: Trajectory of the center of mass, resultant function for φ_1, φ_2 , φ_3 and φ_4.

2.3. Effect of the roller's angle on the angular speed of the wheels for a given trajectory

As the equations have showed so far, the direct as well as the inverse kinematics of the robot can be solved for either a given angular velocity function on the first three wheels or for a given trajectory. A variation in the rollers' angles will undoubtedly affect the trajectory which the robot follows. Nevertheless, if the robot is to achieve the same trajectory every time, a different angle between the wheel axis and that of the rollers will probably affect the angular velocity at which each of them must rotate.

To visualize and confirm this hypothesis, the following test was performed: Given a simple trajectory T: $x - y = 0$ and restricting the angular velocities of the wheels to:

$$\dot{\varphi}_1 = 0, \dot{\varphi}_2 = a_2 t, \dot{\varphi}_3 = a_3 t$$

The coefficients a_2 and a_3 were found as the angle of the rollers were changing in order for the center of mass of the robot to achieve such trajectory T. Then, the distance traveled in either axis (as it is a symmetrical trajectory) was compared to determine in which case the robot had driven a longer distance.

The following table shows the obtained results:

Table 2.1. Results of the test through the trajectory T: $x - y = 0$ for a final time t=10 s

Angle of the roller	a_2	a_3	$x_{t=10\ s} = y_{t=10\ s}$ (mm)
10°	0,2	1,05	49,97
20°	0,285	0,705	71,1
30°	0,31	0,488	77,41
45°	0,5	0,5	124,73
50°	0,527	0,473	131,42
60°	0,559	0,431	139,31
70°	0,5783	0,4227	144,02
80°	0,5603	0,4397	139,43

Figure 2.9 also show the angular velocities found for the fourth wheel. It is interesting to observe that the angle of $45°$ does not require this wheel to move.

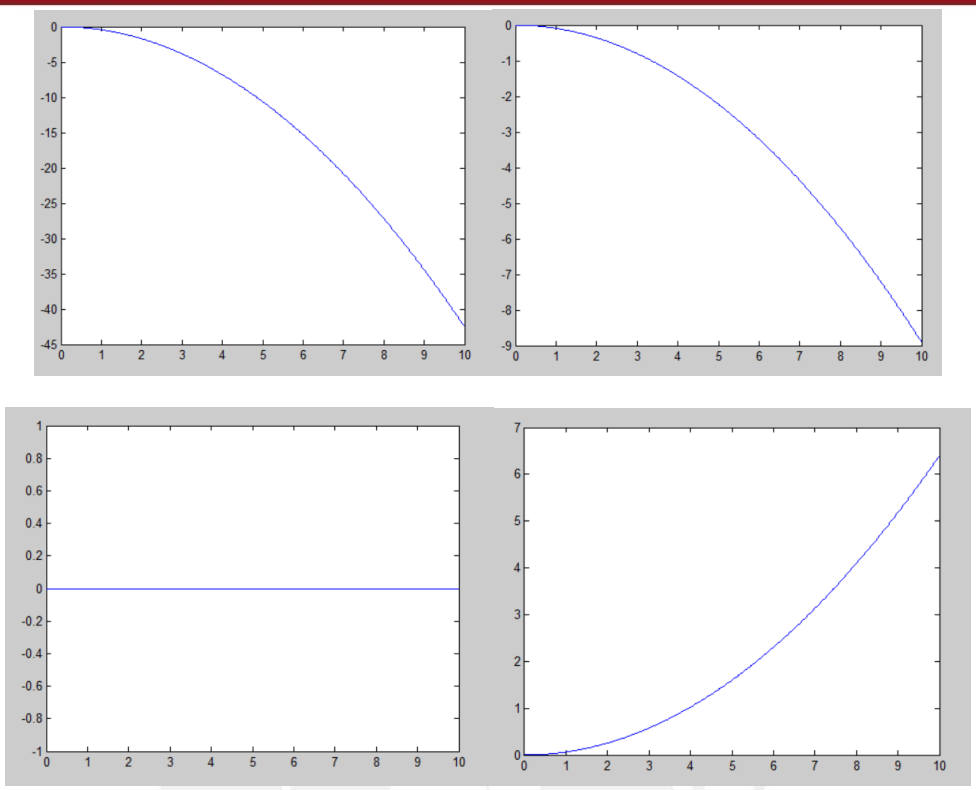

Fig 2.9. From left to right, top to bottom: function $\varphi_4(t)$ for a roller angle of 10º, 30º, 45º and 60º

2.4. Dynamics of the Mecanum-wheeled robot

So far, the kinematics of the Mecanum wheeled robot have been analyzed assuming the velocities of three wheels are given. This is a valid assumption to test the different programs that were written as well as the response of the system to certain input data.

Nevertheless, as these robots are often driven by electric motors, the differential equations that describe the movement of the robot must depend, at the very least, on the torque provided by them.

As the internal forces on the joints of the robot do not require further analysis, an energy method may be used to obtain the differential equations of motion. The second order Lagrange equations with multipliers (as the general case of the robot is described by non-holonomic constraint equations) are used on the entire system, so that the forces and torques that appear internally on the body are neglected.

If a number of n generalized coordinates and r additional constraints are being used to describe the system, the constraint equations that provide consistency, must be homogeneous:

$$f_a^b(\vec{q})\dot{q}^a = 0\,, (a = 1,2,\dots,n\,; b = 1,2,\dots,r), rank(f_a^b) = r$$

Where the vector $\vec{q} = (q^1, q^2, \dots, q^n)$ represents the n coordinates used to describe the system.

Taking this consideration, the Lagrange equations can be written in terms of λ_a coefficients, each one affected by the function f_a^b:

$$\frac{d}{dt}\left(\frac{\partial T}{\partial \dot{q}_a}\right) - \frac{\partial T}{\partial q_a} = Q_a - \lambda_a f_a^b$$

Where Q_a is the generalized force and T is the total kinetic energy of the system.

In the case of the robot, the kinetic energy does not depend directly on the value of the coordinate q_a, from which the equation can be written as:

$$\frac{\partial}{\partial t}\left(\frac{\partial T}{\partial \dot{q}_a}\right) = Q_a - \lambda_a f_a^b$$

The kinetic energy of the robot can be calculated from the linear velocity of each component in it. For this calculation, it will be assumed that the center of mass of the body corresponds to all the elements in the robot except for the wheels.

First, the linear velocities for each component must be calculated. For the first wheel, the following result is obtained:

$$\begin{aligned} v_1^2 &= \dot{x}_{O_1}^2 + \dot{y}_{O_1}^2 \\ &= \dot{x}_G^2 + \dot{y}_G^2 + (l_1^2 + d_1^2)\dot{\psi}^2 + 2\dot{x}_G\dot{\psi}(-l_1\sin(\psi) - d_1\cos(\psi)) \\ &\quad + 2\dot{y}_G\dot{\psi}(l_1\cos(\psi) - d_1\sin(\psi)) \end{aligned}$$

$$\begin{aligned} v_2^2 &= \dot{x}_{O_2}^2 + \dot{y}_{O_2}^2 \\ &= \dot{x}_G^2 + \dot{y}_G^2 + (l_1^2 + d_2^2)\dot{\psi}^2 + 2\dot{x}_G\dot{\psi}(-l_1\sin(\psi) + d_2\cos(\psi)) \\ &\quad + 2\dot{y}_G\dot{\psi}(l_1\cos(\psi) + d_2\sin(\psi)) \end{aligned}$$

$$\begin{aligned} v_3^2 &= \dot{x}_{O_3}^2 + \dot{y}_{O_3}^2 \\ &= \dot{x}_G^2 + \dot{y}_G^2 + (l_2^2 + d_1^2)\dot{\psi}^2 + 2\dot{x}_G\dot{\psi}(l_2\sin(\psi) - d_1\cos(\psi)) \\ &\quad + 2\dot{y}_G\dot{\psi}(-l_2\cos(\psi) - d_1\sin(\psi)) \end{aligned}$$

$$\begin{aligned} v_4^2 &= \dot{x}_{O_4}^2 + \dot{y}_{O_4}^2 \\ &= \dot{x}_G^2 + \dot{y}_G^2 + (l_2^2 + d_2^2)\dot{\psi}^2 + 2\dot{x}_G\dot{\psi}(l_2\sin(\psi) + d_2\cos(\psi)) \\ &\quad + 2\dot{y}_G\dot{\psi}(-l_2\cos(\psi) + d_2\sin(\psi)) \end{aligned}$$

Considering m_w as the mass of each wheel, $J_{w_{22}}$ as the moment of inertia around an axis parallel to the global Z axis and $J_{w_{33}}$ as the moment of inertia around its own geometric axis, the kinetic energy is calculated:

$$T_1 = \frac{1}{2}m_w\Big(\dot{x}_G^2 + \dot{y}_G^2 + (l_1^2 + d_1^2)\dot{\psi}^2 + 2\dot{x}_G\dot{\psi}(-l_1\sin(\psi) - d_1\cos(\psi)) + 2\dot{y}_G\dot{\psi}(l_1\cos(\psi) - d_1\sin(\psi))\Big) + \frac{1}{2}J_{w_{33}}\dot{\varphi}_1^2 + \frac{1}{2}J_{w_{22}}\dot{\psi}^2$$

$$T_2 = \frac{1}{2}m_w\Big(\dot{x}_G^2 + \dot{y}_G^2 + (l_1^2 + d_2^2)\dot{\psi}^2 + 2\dot{x}_G\dot{\psi}(-l_1\sin(\psi) + d_2\cos(\psi)) + 2\dot{y}_G\dot{\psi}(l_1\cos(\psi) + d_2\sin(\psi))\Big) + \frac{1}{2}J_{w_{33}}\dot{\varphi}_2^2 + \frac{1}{2}J_{w_{22}}\dot{\psi}^2$$

$$T_3 = \frac{1}{2}m_w\Big(\dot{x}_G^2 + \dot{y}_G^2 + (l_2^2 + d_1^2)\dot{\psi}^2 + 2\dot{x}_G\dot{\psi}(l_2\sin(\psi) - d_1\cos(\psi)) + 2\dot{y}_G\dot{\psi}(-l_2\cos(\psi) - d_1\sin(\psi))\Big) + \frac{1}{2}J_{w_{33}}\dot{\varphi}_3^2 + \frac{1}{2}J_{w_{22}}\dot{\psi}^2$$

$$T_4 = \frac{1}{2}m_w\Big(\dot{x}_G^2 + \dot{y}_G^2 + (l_2^2 + d_2^2)\dot{\psi}^2 + 2\dot{x}_G\dot{\psi}(l_2\sin(\psi) + d_2\cos(\psi)) + 2\dot{y}_G\dot{\psi}(-l_2\cos(\psi) + d_2\sin(\psi))\Big) + \frac{1}{2}J_{w_{33}}\dot{\varphi}_4^2 + \frac{1}{2}J_{w_{22}}\dot{\psi}^2$$

The kinetic energy of the rest of the robot must also be calculated, considering m_G as the mass and $J_{G_{ZZ}}$ as the moment of inertia around the global Z axis:

$$T_{body} = \frac{1}{2}m_G(\dot{x}_G^2 + \dot{y}_G^2) + \frac{1}{2}J_{G_{ZZ}}\dot{\psi}^2$$

Now, the total energy of the system can be calculated:

$$\begin{aligned} T = \frac{1}{2}(m_G + 4m_w)(\dot{x}_G^2 + \dot{y}_G^2) &+ 2m_w\dot{x}_G\dot{\psi}(-(l_1 - l_2)\sin(\psi) - (d_1 - d_2)\cos(\psi)) \\ &+ 2m_w\dot{y}_G\dot{\psi}\big((l_1 - l_2)\cos(\psi) - (d_1 - d_2)\sin(\psi)\big) \\ &+ \frac{1}{2}J_{w_{33}}(\dot{\varphi}_1^2 + \dot{\varphi}_2^2 + \dot{\varphi}_3^2 + \dot{\varphi}_4^2) + \frac{1}{2}(J_{G_{ZZ}} + 4J_{w_{22}})\dot{\psi}^2 \end{aligned}$$

Partial derivatives of the total energy with respect to the chosen generalized coordinates are required to calculate the equations of motion. For x_G:

$$\frac{\partial T}{\partial \dot{x}_G} = (m_G + 4m_w)\dot{x}_G + 2m_w\dot{\psi}(-(l_1 - l_2)\sin(\psi) - (d_1 - d_2)\cos(\psi))$$

$$\frac{d}{dt}\left(\frac{\partial T}{\partial \dot{x}_G}\right) = (m_G + 4m_w)\ddot{x}_G + 2m_w\ddot{\psi}(-(l_1 - l_2)\sin(\psi) - (d_1 - d_2)\cos(\psi)) + 2m_w\dot{\psi}^2(-(l_1 - l_2)\cos(\psi) + (d_1 - d_2)\sin(\psi))$$

For y_G:

$$\frac{\partial T}{\partial \dot{y}_G} = (m_G + 4m_w)\dot{y}_G + 2m_w\dot{\psi}\big((l_1 - l_2)\cos(\psi) - (d_1 - d_2)\sin(\psi)\big)$$

$$\frac{d}{dt}\left(\frac{\partial T}{\partial \dot{y}_G}\right) = (m_G + 4m_w)\ddot{y}_G + 2m_w\ddot{\psi}\big((l_1 - l_2)\cos(\psi) - (d_1 - d_2)\sin(\psi)\big) + 2m_w\dot{\psi}^2(-(l_1 - l_2)\sin(\psi) - (d_1 - d_2)\cos(\psi))$$

For ψ:

$$\frac{\partial T}{\partial \dot{\psi}} = 2m_w\dot{x}_G(-(l_1 - l_2)\sin(\psi) - (d_1 - d_2)\cos(\psi)) + 2m_w\dot{y}_G\big((l_1 - l_2)\cos(\psi) - (d_1 - d_2)\sin(\psi)\big) + (J_{G_{ZZ}} + 4J_{w_{22}})\dot{\psi}$$

$$\frac{d}{dt}\left(\frac{\partial T}{\partial \dot{\psi}}\right) = 2m_w\ddot{x}_G(-(l_1 - l_2)\sin(\psi) - (d_1 - d_2)\cos(\psi)) + 2m_w\ddot{y}_G\big((l_1 - l_2)\cos(\psi) - (d_1 - d_2)\sin(\psi)\big) + 2m_w\dot{x}_G\dot{\psi}(-(l_1 - l_2)\cos(\psi) + (d_1 - d_2)\sin(\psi)) + 2m_w\dot{y}_G\dot{\psi}(-(l_1 - l_2)\sin(\psi) - (d_1 - d_2)\cos(\psi)) + (J_{G_{ZZ}} + 4J_{w_{22}})\ddot{\psi}$$

For φ_i, with $i = 1,2,3,4$:

$$\frac{\partial T}{\partial \dot{\varphi}_i} = J_{w_{33}}\dot{\varphi}_i$$

$$\frac{d}{dt}\left(\frac{\partial T}{\partial \dot{\varphi}_i}\right) = J_{w_{33}}\ddot{\varphi}_i$$

The constraint equations play an important role, as they define the functions that multiply each λ_i coefficient:

$$\dot{x_G}\sin(\psi + \delta_1) - \dot{y_G}\cos(\psi + \delta_1) - l_1\dot{\psi}\cos(\delta_1) - d_1\dot{\psi}\sin(\delta_1) - R\dot{\varphi_1}\sin(\delta_1) = 0$$

$$\dot{x_G}\sin(\psi + \delta_2) - \dot{y_G}\cos(\psi + \delta_2) - l_1\dot{\psi}\cos(\delta_2) + d_2\dot{\psi}\sin(\delta_2) - R\dot{\varphi_2}\sin(\delta_2) = 0$$

$$\dot{x_G}\sin(\psi + \delta_3) - \dot{y_G}\cos(\psi + \delta_3) + l_2\dot{\psi}\cos(\delta_3) - d_1\dot{\psi}\sin(\delta_3) - R\dot{\varphi_3}\sin(\delta_3) = 0$$

$$\dot{x_G}\sin(\psi+\delta_4)-\dot{y_G}\cos(\psi+\delta_4)+l_2\dot{\psi}\cos(\delta_4)+d_2\dot{\psi}\sin(\delta_4)-R\dot{\varphi_4}\sin(\delta_4)=0$$

Finally, the Lagrange equations with multipliers can be written as follows:

$$\begin{aligned}(m_G+4m_w)\ddot{x}_G+2m_w\ddot{\psi}(-(l_1-l_2)\sin(\psi)-(d_1-d_2)\cos(\psi))\\+2m_w\dot{\psi}^2(-(l_1-l_2)\cos(\psi)+(d_1-d_2)\sin(\psi))\\=\lambda_1\sin(\psi+\delta_1)+\lambda_2\sin(\psi+\delta_2)+\lambda_3\sin(\psi+\delta_3)\\+\lambda_4\sin(\psi+\delta_4)\end{aligned}\quad(1)$$

$$\begin{aligned}(m_G+4m_w)\ddot{y}_G+2m_w\ddot{\psi}\big((l_1-l_2)\cos(\psi)-(d_1-d_2)\sin(\psi)\big)\\+2m_w\dot{\psi}^2(-(l_1-l_2)\sin(\psi)-(d_1-d_2)\cos(\psi))\\=-\lambda_1\cos(\psi+\delta_1)-\lambda_2\cos(\psi+\delta_2)-\lambda_3\cos(\psi+\delta_3)\\-\lambda_4\cos(\psi+\delta_4)\end{aligned}\quad(2)$$

$$\begin{aligned}2m_w\ddot{x}_G(-(l_1-l_2)\sin(\psi)-(d_1-d_2)\cos(\psi))\\+2m_w\ddot{y}_G\big((l_1-l_2)\cos(\psi)-(d_1-d_2)\sin(\psi)\big)\\+2m_w\dot{x}_G\dot{\psi}(-(l_1-l_2)\cos(\psi)+(d_1-d_2)\sin(\psi))\\+2m_w\dot{y}_G\dot{\psi}(-(l_1-l_2)\sin(\psi)-(d_1-d_2)\cos(\psi))\\+\big(J_{G_{ZZ}}+4J_{w_{22}}\big)\ddot{\psi}\\=\lambda_1(-l_1\cos(\delta_1)-d_1\sin(\delta_1))\\+\lambda_2(-l_1\cos(\delta_2)+d_2\sin(\delta_2))\\+\lambda_3(l_2\cos(\delta_3)-d_1\sin(\delta_3))\\+\lambda_4(l_2\cos(\delta_4)+d_2\sin(\delta_4))\end{aligned}\quad(3)$$

$$J_{w_{33}}\ddot{\varphi}_1=M_1(t)-\lambda_1\mathrm{R}\sin(\delta_1)\quad(4)$$

$$J_{w_{33}}\ddot{\varphi}_2=M_2(t)-\lambda_2\mathrm{R}\sin(\delta_2)\quad(5)$$

$$J_{w_{33}}\ddot{\varphi}_3=M_3(t)-\lambda_3\mathrm{R}\sin(\delta_3)\quad(6)$$

$$J_{w_{33}}\ddot{\varphi}_4=M_4(t)-\lambda_4\mathrm{R}\sin(\delta_4)\quad(7)$$

From equations (4) through (7), the four coefficients can be calculated:

$$\lambda_i=\frac{M_i(t)-J_{w_{33}}\ddot{\varphi}_i}{R\sin(\delta_i)}$$

For $i=1,2,3,4$

Finally, to solve the system, the functions $\ddot{\varphi}_i$ must be calculated in terms of the other generalized coordinates. This can be achieved through the examination of the constraint equations and further derivation with respect to time:

$$\ddot{\varphi}_1 = \frac{\ddot{x}_G \sin(\psi + \delta_1) - \ddot{y}_G \cos(\psi + \delta_1) + \ddot{\psi}(-l_1 \cos(\delta_1) - d_1 \sin(\delta_1)) + \dot{x}_G \dot{\psi} \cos(\psi + \delta_1)}{R \sin(\delta_1)}$$

$$\ddot{\varphi}_2 = \frac{\ddot{x}_G \sin(\psi + \delta_2) - \ddot{y}_G \cos(\psi + \delta_2) + \ddot{\psi}(-l_1 \cos(\delta_2) + d_2 \sin(\delta_2)) + \dot{x}_G \dot{\psi} \cos(\psi + \delta_2)}{R \sin(\delta_2)}$$

$$\ddot{\varphi}_3 = \frac{\ddot{x}_G \sin(\psi + \delta_3) - \ddot{y}_G \cos(\psi + \delta_3) + \ddot{\psi}(l_2 \cos(\delta_3) - d_1 \sin(\delta_3)) + \dot{x}_G \dot{\psi} \cos(\psi + \delta_3) +}{R \sin(\delta_3)}$$

$$\ddot{\varphi}_4 = \frac{\ddot{x}_G \sin(\psi + \delta_4) - \ddot{y}_G \cos(\psi + \delta_4) + \ddot{\psi}(l_2 \cos(\delta_4) + d_2 \sin(\delta_4)) + \dot{x}_G \dot{\psi} \cos(\psi + \delta_4) +}{R \sin(\delta_4)}$$

Replacing the values for $\ddot{\varphi}_i$ in equations (1) through (3) and rearranging the terms, the following system of equations is obtained:

$$a_{11}\ddot{x}_G + a_{12}\ddot{y}_G + a_{13}\ddot{\psi} + a_{14}\dot{x}_G\dot{\psi} + a_{15}\dot{y}_G\dot{\psi} + a_{16}\dot{\psi}^2 = f_1(t,\psi) \quad (8)$$

$$a_{21}\ddot{x}_G + a_{22}\ddot{y}_G + a_{23}\ddot{\psi} + a_{24}\dot{x}_G\dot{\psi} + a_{25}\dot{y}_G\dot{\psi} + a_{26}\dot{\psi}^2 = f_2(t,\psi) \quad (9)$$

$$a_{31}\ddot{x}_G + a_{32}\ddot{y}_G + a_{33}\ddot{\psi} + a_{34}\dot{x}_G\dot{\psi} + a_{35}\dot{y}_G\dot{\psi} = f_3(t,\psi) \quad (10)$$

Where the functions $f_i(t,\psi)$ are:

$$f_1(t,\psi) = \sum_{i=1}^{4} \frac{M_i(t) \sin(\psi + \delta_i)}{R \sin(\delta_i)}$$

$$f_2(t,\psi) = -\sum_{i=1}^{4} \frac{M_i(t) \cos(\psi + \delta_i)}{R \sin(\delta_i)}$$

$$f_3(t,\psi) = \frac{M_1(t)(-l_1\cos(\delta_1) - d_1\sin(\delta_1))}{R\sin(\delta_1)} + \frac{M_2(t)(-l_1\cos(\delta_2) + d_2\sin(\delta_2))}{R\sin(\delta_2)} + \frac{M_3(t)(l_2\cos(\delta_3) - d_1\sin(\delta_3))}{R\sin(\delta_3)} + \frac{M_4(t)(l_2\cos(\delta_4) + d_2\sin(\delta_4))}{R\sin(\delta_4)}$$

And the coefficients a_{ij} are:

$$a_{11} = m_G + 4m_w + \frac{J_{w_{33}}}{R^2}\left(\frac{\sin^2(\psi+\delta_1)}{\sin^2(\delta_1)} + \frac{\sin^2(\psi+\delta_2)}{\sin^2(\delta_2)} + \frac{\sin^2(\psi+\delta_3)}{\sin^2(\delta_3)} + \frac{\sin^2(\psi+\delta_4)}{\sin^2(\delta_4)}\right)$$

$$a_{12} = -\frac{J_{w_{33}}}{R^2}\left(\frac{\sin(\psi+\delta_1)\cos(\psi+\delta_1)}{\sin^2(\delta_1)} + \frac{\sin(\psi+\delta_2)\cos(\psi+\delta_2)}{\sin^2(\delta_2)} + \frac{\sin(\psi+\delta_3)\cos(\psi+\delta_3)}{\sin^2(\delta_3)} + \frac{\sin(\psi+\delta_4)\cos(\psi+\delta_4)}{\sin^2(\delta_4)}\right)$$

$$a_{13} = 2m_w(-(l_1-l_2)\sin(\psi) - (d_1-d_2)\cos(\psi)) + \frac{J_{w_{33}}}{R^2}\left(\frac{\sin(\psi+\delta_1)\,(-l_1\cos(\delta_1) - d_1\sin(\delta_1))}{\sin^2(\delta_1)} + \frac{\sin(\psi+\delta_2)\,(-l_1\cos(\delta_2) + d_2\sin(\delta_2))}{\sin^2(\delta_2)} + \frac{\sin(\psi+\delta_3)\,(l_2\cos(\delta_3) - d_1\sin(\delta_3))}{\sin^2(\delta_3)} + \frac{\sin(\psi+\delta_4)\,(l_2\cos(\delta_4) + d_2\sin(\delta_4))}{\sin^2(\delta_4)}\right)$$

$$a_{14} = \frac{J_{w_{33}}}{R^2}\left(\frac{\sin(\psi+\delta_1)\cos(\psi+\delta_1)}{\sin^2(\delta_1)} + \frac{\sin(\psi+\delta_2)\cos(\psi+\delta_2)}{\sin^2(\delta_2)} + \frac{\sin(\psi+\delta_3)\cos(\psi+\delta_3)}{\sin^2(\delta_3)} + \frac{\sin(\psi+\delta_4)\cos(\psi+\delta_4)}{\sin^2(\delta_4)}\right)$$

$$a_{15} = \frac{J_{w_{33}}}{R^2}\left(\frac{\sin^2(\psi+\delta_1)}{\sin^2(\delta_1)} + \frac{\sin^2(\psi+\delta_2)}{\sin^2(\delta_2)} + \frac{\sin^2(\psi+\delta_3)}{\sin^2(\delta_3)} + \frac{\sin^2(\psi+\delta_4)}{\sin^2(\delta_4)}\right)$$

$$a_{16} = 2m_w(-(l_1 - l_2)\cos(\psi) + (d_1 - d_2)\sin(\psi))$$

$$a_{21} = -\frac{J_{w_{33}}}{R^2}\left(\frac{\sin(\psi+\delta_1)\cos(\psi+\delta_1)}{\sin^2(\delta_1)} + \frac{\sin(\psi+\delta_2)\cos(\psi+\delta_2)}{\sin^2(\delta_2)} + \frac{\sin(\psi+\delta_3)\cos(\psi+\delta_3)}{\sin^2(\delta_3)} + \frac{\sin(\psi+\delta_4)\cos(\psi+\delta_4)}{\sin^2(\delta_4)}\right)$$

$$a_{22} = m_G + 4m_w + \frac{J_{w_{33}}}{R^2}\left(\frac{\cos^2(\psi+\delta_1)}{\sin^2(\delta_1)} + \frac{\cos^2(\psi+\delta_2)}{\sin^2(\delta_2)} + \frac{\cos^2(\psi+\delta_3)}{\sin^2(\delta_3)} + \frac{\cos^2(\psi+\delta_4)}{\sin^2(\delta_4)}\right)$$

$$a_{23} = 2m_w\big((l_1 - l_2)\cos(\psi) - (d_1 - d_2)\sin(\psi)\big) - \frac{J_{w_{33}}}{R^2}\left(\frac{\cos(\psi+\delta_1)\,(-l_1\cos(\delta_1) - d_1\sin(\delta_1))}{\sin^2(\delta_1)} + \frac{\cos(\psi+\delta_2)\,(-l_1\cos(\delta_2) + d_2\sin(\delta_2))}{\sin^2(\delta_2)} + \frac{\cos(\psi+\delta_3)\,(l_2\cos(\delta_3) - d_1\sin(\delta_3))}{\sin^2(\delta_3)} + \frac{\cos(\psi+\delta_4)\,(l_2\cos(\delta_4) + d_2\sin(\delta_4))}{\sin^2(\delta_4)}\right)$$

$$a_{24} = -\frac{J_{w_{33}}}{R^2}\left(\frac{\cos^2(\psi+\delta_1)}{\sin^2(\delta_1)} + \frac{\cos^2(\psi+\delta_2)}{\sin^2(\delta_2)} + \frac{\cos^2(\psi+\delta_3)}{\sin^2(\delta_3)} + \frac{\cos^2(\psi+\delta_4)}{\sin^2(\delta_4)}\right)$$

$$a_{25} = -\frac{J_{w_{33}}}{R^2}\left(\frac{\sin(\psi+\delta_1)\cos(\psi+\delta_1)}{\sin^2(\delta_1)} + \frac{\sin(\psi+\delta_2)\cos(\psi+\delta_2)}{\sin^2(\delta_2)} + \frac{\sin(\psi+\delta_3)\cos(\psi+\delta_3)}{\sin^2(\delta_3)} + \frac{\sin(\psi+\delta_4)\cos(\psi+\delta_4)}{\sin^2(\delta_4)}\right)$$

$$a_{26} = 2m_w(-(l_1 - l_2)\sin(\psi) - (d_1 - d_2)\cos(\psi))$$

$$\begin{aligned} a_{31} = {} & 2m_w(-(l_1 - l_2)\sin(\psi) - (d_1 - d_2)\cos(\psi)) \\ & + \frac{J_{w_{33}}}{R^2}\left(\frac{\sin(\psi + \delta_1)\,(-l_1\cos(\delta_1) - d_1\sin(\delta_1))}{\sin^2(\delta_1)}\right. \\ & + \frac{\sin(\psi + \delta_2)\,(-l_1\cos(\delta_2) + d_2\sin(\delta_2))}{\sin^2(\delta_2)} \\ & + \frac{\sin(\psi + \delta_3)\,(l_2\cos(\delta_3) - d_1\sin(\delta_3))}{\sin^2(\delta_3)} \\ & \left. + \frac{\sin(\psi + \delta_4)\,(l_2\cos(\delta_4) + d_2\sin(\delta_4))}{\sin^2(\delta_4)}\right) \end{aligned}$$

$$\begin{aligned} a_{32} = {} & 2m_w\big((l_1 - l_2)\cos(\psi) - (d_1 - d_2)\sin(\psi)\big) \\ & - \frac{J_{w_{33}}}{R^2}\left(\frac{\cos(\psi + \delta_1)\,(-l_1\cos(\delta_1) - d_1\sin(\delta_1))}{\sin^2(\delta_1)}\right. \\ & + \frac{\cos(\psi + \delta_2)\,(-l_1\cos(\delta_2) + d_2\sin(\delta_2))}{\sin^2(\delta_2)} \\ & + \frac{\cos(\psi + \delta_3)\,(l_2\cos(\delta_3) - d_1\sin(\delta_3))}{\sin^2(\delta_3)} \\ & \left. + \frac{\cos(\psi + \delta_4)\,(l_2\cos(\delta_4) + d_2\sin(\delta_4)}{\sin^2(\delta_4)}\right) \end{aligned}$$

$$\begin{aligned} a_{33} = {} & J_{G_{zz}} + 4J_{w_{22}} \\ & + \frac{J_{w_{33}}}{R^2}\left(\frac{(-l_1\cos(\delta_1) - d_1\sin(\delta_1))^2}{\sin^2(\delta_1)} + \frac{(-l_1\cos(\delta_2) + d_2\sin(\delta_2))^2}{\sin^2(\delta_2)}\right. \\ & \left. + \frac{(l_2\cos(\delta_3) - d_1\sin(\delta_3))^2}{\sin^2(\delta_3)} + \frac{(l_2\cos(\delta_4) + d_2\sin(\delta_4))^2}{\sin^2(\delta_4)}\right) \end{aligned}$$

$$a_{34} = 2m_w(-(l_1 - l_2)\cos(\psi) - (d_1 - d_2)\sin(\psi)) + \frac{J_{w_{33}}}{R^2}\left(\frac{\cos(\psi + \delta_1)\,(-l_1\cos(\delta_1) - d_1\sin(\delta_1))}{\sin^2(\delta_1)} + \frac{\cos(\psi + \delta_2)\,(-l_1\cos(\delta_2) + d_2\sin(\delta_2))}{\sin^2(\delta_2)} + \frac{\cos(\psi + \delta_3)\,(l_2\cos(\delta_3) - d_1\sin(\delta_3))}{\sin^2(\delta_3)} + \frac{\cos(\psi + \delta_4)\,(l_2\cos(\delta_4) + d_2\sin(\delta_4))}{\sin^2(\delta_4)}\right)$$

$$a_{35} = 2m_w(-(l_1 - l_2)\sin(\psi) - (d_1 - d_2)\cos(\psi)) + \frac{J_{w_{33}}}{R^2}\left(\frac{\sin(\psi + \delta_1)\,(-l_1\cos(\delta_1) - d_1\sin(\delta_1))}{\sin^2(\delta_1)} + \frac{\sin(\psi + \delta_2)\,(-l_1\cos(\delta_2) + d_2\sin(\delta_2))}{\sin^2(\delta_2)} + \frac{\sin(\psi + \delta_3)\,(l_2\cos(\delta_3) - d_1\sin(\delta_3))}{\sin^2(\delta_3)} + \frac{\sin(\psi + \delta_4)\,(l_2\cos(\delta_4) + d_2\sin(\delta_4))}{\sin^2(\delta_4)}\right)$$

Equations [8] through [10] stablish a system of second order nonlinear ordinary differential equations, for which the fourth order Runge-Kutta method will be used to solve it. However, this requires an additional step in order to transform the second order differential equations into first order. The following change of variables becomes necessary:

$$\dot{x}_G = u \rightarrow \ddot{x}_G = \dot{u};\ \dot{x}_G(0) = u(0)$$

$$\dot{y}_G = v \rightarrow \ddot{y}_G = \dot{v};\ \dot{y}_G(0) = v(0)$$

$$\dot{\psi} = w \rightarrow \ddot{\psi} = \dot{w};\ \dot{\psi}(0) = w(0)$$

Thus, resulting in the following system:

$$a_{11}\dot{u} + a_{12}\dot{v} + a_{13}\dot{w} = f_1(t,\psi) - (a_{14}uw + a_{15}vw + a_{16}w^2) \quad (11)$$

$$a_{21}\dot{u} + a_{22}\dot{v} + a_{23}\dot{w} = f_2(t,\psi) - (a_{24}uw + a_{25}vw + a_{26}w^2) \quad (12)$$

$$a_{31}\dot{u} + a_{32}\dot{v} + a_{33}\dot{w} = f_3(t,\psi) - (a_{34}uw + a_{35}vw) \quad (13)$$

Writing the complete system using matrix notation:

$$\begin{bmatrix} a_{11} & a_{12} & a_{13} & 0 & 0 & 0 \\ a_{21} & a_{22} & a_{23} & 0 & 0 & 0 \\ a_{31} & a_{32} & a_{33} & 0 & 0 & 0 \\ 0 & 0 & 0 & 1 & 0 & 0 \\ 0 & 0 & 0 & 0 & 1 & 0 \\ 0 & 0 & 0 & 0 & 0 & 1 \end{bmatrix} \cdot \begin{bmatrix} \dot{u} \\ \dot{v} \\ \dot{w} \\ \dot{x}_G \\ \dot{y}_G \\ \dot{\psi} \end{bmatrix} = \begin{bmatrix} f_1(t,\psi) - (a_{14}uw + a_{15}vw + a_{16}w^2) \\ f_2(t,\psi) - (a_{24}uw + a_{25}vw + a_{26}w^2) \\ f_3(t,\psi) - (a_{34}uw + a_{35}vw) \\ u \\ v \\ w \end{bmatrix}$$

The system can now be solved using the Runge-Kutta method for different functions $M_i(t)$ to obtain $x_G(t)$, $y_G(t)$ and $\psi(t)$.

Different trajectories of the center of mass (x_G, y_G) are presented in the following graphics, which correspond to different functions $M_i(t)$. All the inertial parameters (mass and moment of inertia) are taken as the unit.

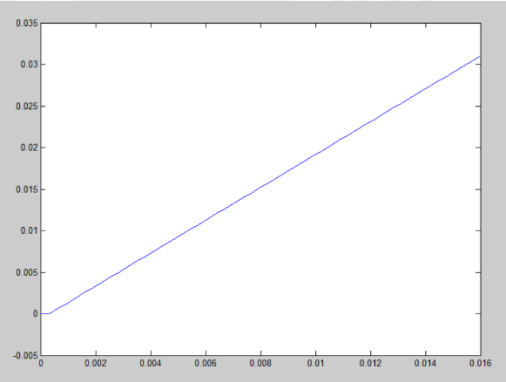

Fig 2.10. Trajectory of the center of mass for $M_1 = M_2 = M_3 = M_4 = 1\ N.mm$

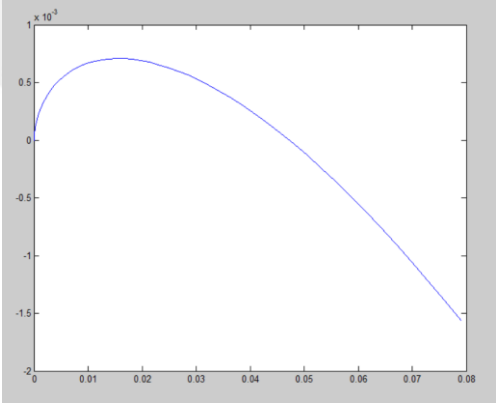

Fig 2.11. Trajectory of the center of mass for $M_1 = M_2 = M_3 = M_4 = t\ [N.mm]$

2.5. Inverse kinematics and optimization of driving torques for a specific robot

So far, the direct kinematics of the system were solved, as the torque functions were already given. The inverse kinematics problem, however, cannot be easily solved, as from

a given trajectory only $x_G(t)$, $y_G(t)$ and $\psi(t)$ and its derivatives can be calculated, but the system still lacks a fourth equation which would allow the calculation of the four torque functions. Physically, this means that there exists an infinite combination of functions $M_i(t)$, which can together achieve the given trajectory.

From the mechanical point of view, the fact of posing a fourth equation on the system would mean that an additional restriction must be given to it. To take advantage of this equation, the restriction must be such, that the total energy consumed by the robot to follow a given trajectory must be a minimum.

For the case of a DC motor, the torque is linearly dependent on the voltage (Gorinevsky: 1997) , meaning that:

$$M_i = C_u U_i - C_v \dot{\varphi}_i$$

With C_u and C_v being constants which depend on the characteristics of the motor. In particular, they depend on the nominal torque M_n, the nominal angular velocity ω_n , the nominal tension U_n and the starting torque M_1:

$$C_u = \frac{M_1}{U_n}$$

$$C_v = \frac{(M_1 - M_n)}{\omega_n}$$

For example, the Maxon Motor DC-Max 16 S has the following characteristics:

$$U_n = 6\,V\ ;\ M_n = 4{,}04\,mN \cdot m\ ;\ \omega_n = 506{,}8\frac{rad}{s}\ ;\ M_1 = 10{,}5\ mN \cdot m$$

Hence, the values for the coefficients C_u and C_v are:

$$C_u = 1{,}75\ \frac{N}{V}\ ;\ C_v = \ 0{,}013\ N \cdot s$$

It is also known that power consumed in a DC motor is proportional to the square of the voltage:

$$P\ \alpha\ U_i^2$$

From this, it can be inferred that the power is also proportional to the square of the torque.

$$P \, \alpha \, M_i^2$$

Thus, the energy consumed by the robot will be minimized if the sum $\sum_{i=1}^{4} M_i^2$ can be also minimized. This constitutes an additional restriction to the system, which means the functions $M_i(t)$ can be fully defined for a given trajectory.

In this study, the general equations, which were found in previous analysis, will be reduced doing the following considerations:

$$\delta_1 = \delta_4 = -\delta_2 = -\delta_3 = 45º$$

$$l_1 = l_2 = l \; ; \; d_1 = d_2 = d$$

In addition, the following terms will be defined:

$$m = m_G + 4m_w$$

$$J_c = J_{G_{zz}} + 4J_{w_{22}} + 4m_w(l^2 + d^2)$$

And to simplify the notation, $M_i(t) = M_i$. This does not mean in any way that the driving torque is constant.

Simplifying the differential equations of motion:

$$\ddot{x}_G \left(m + \frac{4J_{w_{33}}}{R^2}\right) = -\frac{4J_{w_{33}}}{R^2}\dot{y}_G\dot{\psi} + \frac{\cos(\psi) + \sin(\psi)}{R}(M_1 + M_4) + \frac{\cos(\psi) - \sin(\psi)}{R}(M_2 + M_3) \tag{14}$$

$$\ddot{y}_G \left(m + \frac{4J_{w_{33}}}{R^2}\right) = \frac{4J_{w_{33}}}{R^2}\dot{x}_G\dot{\psi} - \frac{\cos(\psi) - \sin(\psi)}{R}(M_1 + M_4) + \frac{\cos(\psi) + \sin(\psi)}{R}(M_2 + M_3) \tag{15}$$

$$\ddot{\psi}\left(J_c + \frac{4J_{w_{33}}}{R^2}(l^2 + d^2)\right) = \frac{l + d}{R}(M_2 - M_1 + M_3 - M_4) \tag{16}$$

In order to calculate de torque functions, the functions M_i must be expressed in terms of the generalized coordinates. Equations (14) through (16) can be rearranged as:

$$M_2 + M_3 = \frac{R\sqrt{2}}{2}\left(\left(\ddot{x}_G\left(m + \frac{4J_{w_{33}}}{R^2}\right) + \frac{4J_{w_{33}}}{R^2}\dot{y}_G\dot{\psi}\right)\cos\left(\psi + \frac{\pi}{4}\right) + \left(\ddot{y}_G\left(m + \frac{4J_{w_{33}}}{R^2}\right) - \frac{4J_{w_{33}}}{R^2}\dot{x}_G\dot{\psi}\right)\sin\left(\psi + \frac{\pi}{4}\right)\right)$$

$$M_1 + M_4 = \frac{R\sqrt{2}}{2}\left(\left(\ddot{x}_G\left(m + \frac{4J_{w_{33}}}{R^2}\right) + \frac{4J_{w_{33}}}{R^2}\dot{y}_G\dot{\psi}\right)\sin\left(\psi + \frac{\pi}{4}\right) - \left(\ddot{y}_G\left(m + \frac{4J_{w_{33}}}{R^2}\right) - \frac{4J_{w_{33}}}{R^2}\dot{x}_G\dot{\psi}\right)\cos\left(\psi + \frac{\pi}{4}\right)\right)$$

$$M_2 - M_1 + M_3 - M_4 = \frac{R}{l+d}\ddot{\psi}\left(J_c + \frac{4J_{w_{33}}}{R^2}(l^2 + d^2)\right)$$

Conveniently, the equations have been arranged in such a way that allows the manipulation of all torque functions as dependent on the generalized coordinates. Moreover:

$$M_2 + M_3 = A$$

$$M_1 + M_4 = B$$

$$M_2 - M_1 + M_4 - M_3 = C$$

With:

$$A = \frac{R\sqrt{2}}{2}\left(\left(\ddot{x}_G\left(m + \frac{4J_{w_{33}}}{R^2}\right) + \frac{4J_{w_{33}}}{R^2}\dot{y}_G\dot{\psi}\right)\cos\left(\psi + \frac{\pi}{4}\right) + \left(\ddot{y}_G\left(m + \frac{4J_{w_{33}}}{R^2}\right) - \frac{4J_{w_{33}}}{R^2}\dot{x}_G\dot{\psi}\right)\sin\left(\psi + \frac{\pi}{4}\right)\right)$$

$$B = \frac{R\sqrt{2}}{2}\left(\left(\ddot{x}_G\left(m + \frac{4J_{w_{33}}}{R^2}\right) + \frac{4J_{w_{33}}}{R^2}\dot{y}_G\dot{\psi}\right)\sin\left(\psi + \frac{\pi}{4}\right)\right.$$
$$\left. - \left(\ddot{y}_G\left(m + \frac{4J_{w_{33}}}{R^2}\right) - \frac{4J_{w_{33}}}{R^2}\dot{x}_G\dot{\psi}\right)\cos\left(\psi + \frac{\pi}{4}\right)\right)$$

$$C = \frac{R}{l+d}\ddot{\psi}\left(J_c + \frac{4J_{w_{33}}}{R^2}(l^2 + d^2)\right)$$

It is evident here that the only way to solve the system is by imposing an additional restriction. The system can be arranged so that all depends on one single torque:

$$M_2 + M_3 = A \tag{17}$$

$$M_1 = B - M_4 \tag{18}$$

$$M_2 - M_1 - M_3 = C - M_4 \tag{19}$$

Solving the equations (17), (18) and (19) for M_1, M_2 and M_3:

$$M_1 = B - M_4$$

$$M_2 = \frac{A + B + C}{2} - M_4$$

$$M_3 = \frac{A - B - C}{2} + M_4$$

Imposing now the energy condition, the function to minimize should be:

$$P(t) = M_T^2 = M_1^2 + M_2^2 + M_3^2 + M_4^2$$

Replacing the function in terms of M_4:

$$P(t) = (B - M_4)^2 + \left(\frac{A + B + C}{2} - M_4\right)^2 + \left(\frac{A - B - C}{2} + M_4\right)^2 + M_4^2$$

To find the minimum, the derivative of $P(t)$ with respect to M_4 must be equal to zero:

$$\frac{dP(t)}{dM_4} = 0$$

$$M_{4_{min}} = \frac{B}{2} + \frac{C}{4}$$

Which is the value of M_4 for a given trajectory, which minimizes the energy added to the system. The remaining values of the driving torques can be also calculated:

$$M_{1_{min}} = \frac{B}{2} - \frac{C}{4}$$

$$M_{2_{min}} = \frac{A}{2} + \frac{C}{4}$$

$$M_{3_{min}} = \frac{A}{2} - \frac{C}{4}$$

Several driving torque functions can be calculated for different trajectories of the center of mass, as shown in the following pictures:

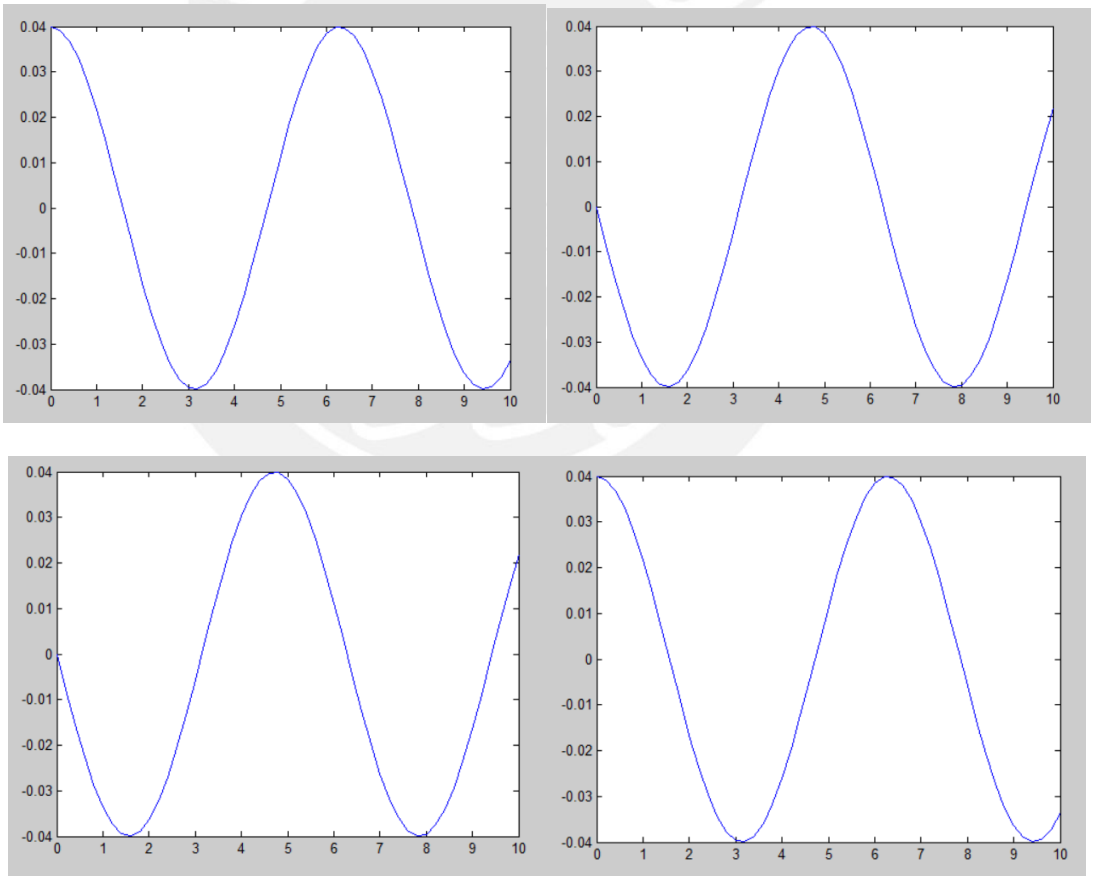

Figure 11. From top to bottom, left to right: Driving torques M_1, M_2, M_3 and M_4 for a trajectory $x = y = t$

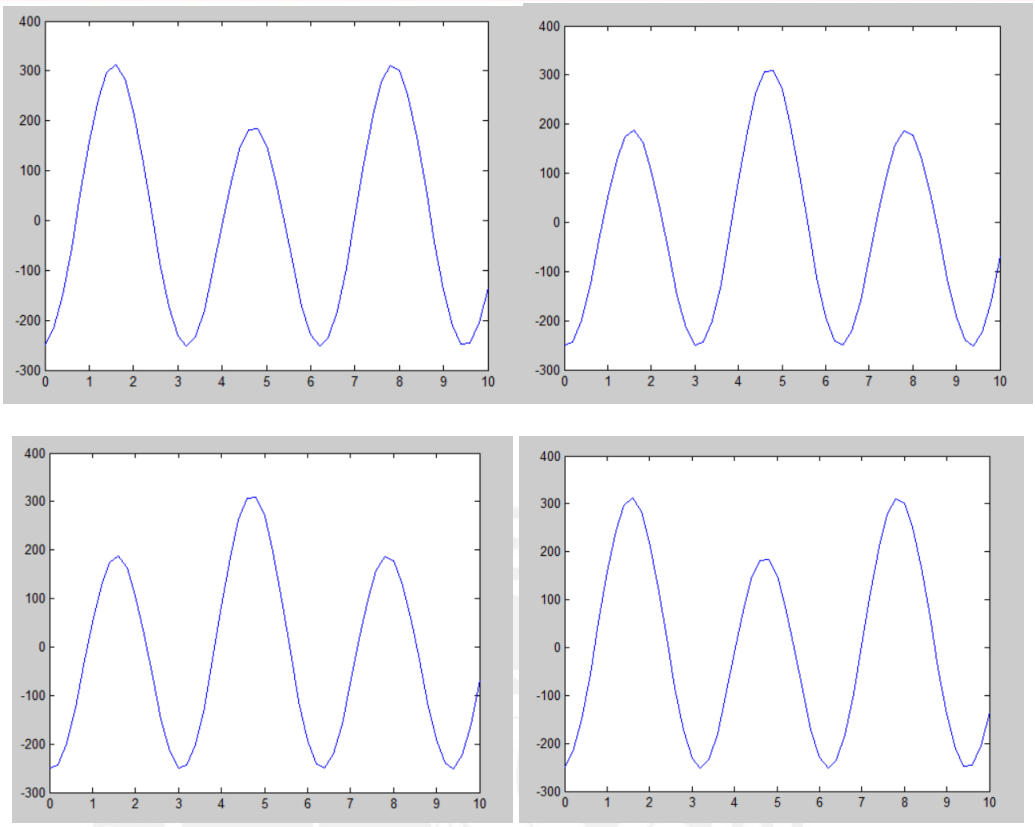

Figure 2.12. From top to bottom, left to right: Driving torques M_1, M_2, M_3 and M_4 for a trajectory $x = \cos(2t)$, $y = \sin(t)$

In spite of all the equations developed so far, in a real mechatronic system, the variable which is usually controlled is the voltage signal U_i on each motor. This fact poses the need to develop equations that will allow controlling such signal for any given trajectory.

It was mentioned earlier that the equation for the torque provided by a DC motor was the following:

$$M_i = C_u U_i - C_v \dot{\varphi}_i$$

This relation can be easily replaced in equations (*), (**) and (***) to establish a relation between the voltage and the generalized coordinates. It will be assumed that all motors have the same characteristics:

$$C_u(U_2 + U_3) - C_v(\dot{\varphi}_2 + \dot{\varphi}_3) = A$$

$$C_u(U_1 + U_4) - C_v(\dot{\varphi}_1 + \dot{\varphi}_4) = B$$

$$C_u(U_2 - U_1 + U_4 - U_3) - C_v(\dot{\varphi}_2 - \dot{\varphi}_1 + \dot{\varphi}_4 - \dot{\varphi}_3) = C$$

Leaving all the voltage signals on the left side of the equation:

$$U_2 + U_3 = \frac{A}{C_u} + \frac{C_v}{C_u}(\dot{\varphi}_2 + \dot{\varphi}_3)$$

$$U_1 + U_4 = \frac{B}{C_u} + \frac{C_v}{C_u}(\dot{\varphi}_1 + \dot{\varphi}_4)$$

$$U_2 - U_1 + U_4 - U_3 = \frac{C}{C_u} + \frac{C_v}{C_u}(\dot{\varphi}_2 - \dot{\varphi}_1 + \dot{\varphi}_4 - \dot{\varphi}_3)$$

As it can be recalled, the terms A, B and C are functions of the generalized coordinates. The missing relationship between the wheels angular velocity $\dot{\varphi}_i$ and the kinematic variables is given by the constraint equations. For this particular case, they are simplified to:

$$\dot{\varphi}_1 = \frac{\dot{x}_G(\cos(\psi) + \sin(\psi)) - \dot{y}_G(\cos(\psi) - \sin(\psi)) - \dot{\psi}(l + d)}{R}$$

$$\dot{\varphi}_2 = \frac{\dot{x}_G(\cos(\psi) - \sin(\psi)) + \dot{y}_G(\cos(\psi) + \sin(\psi)) + \dot{\psi}(l + d)}{R}$$

$$\dot{\varphi}_3 = \frac{\dot{x}_G(\cos(\psi) - \sin(\psi)) + \dot{y}_G(\cos(\psi) + \sin(\psi)) - \dot{\psi}(l + d)}{R}$$

$$\dot{\varphi}_4 = \frac{\dot{x}_G(\cos(\psi) + \sin(\psi)) + \dot{y}_G(\sin(\psi) - \cos(\psi)) + \dot{\psi}(l + d)}{R}$$

The right hand of the 3 voltage equations can be the written as new terms A', B' and C', which are all functions of the generalized coordinates:

$$U_2 + U_3 = A'$$

$$U_1 + U_4 = B'$$

$$U_2 - U_1 + U_4 - U_3 = C'$$

Where:

$$A' = \frac{A}{C_u} + \frac{C_v}{C_u}(\dot{\varphi}_2 + \dot{\varphi}_3)$$

$$B' = \frac{B}{C_u} + \frac{C_v}{C_u}(\dot{\varphi}_1 + \dot{\varphi}_4)$$

$$C' = \frac{C}{C_u} + \frac{C_v}{C_u}(\dot{\varphi}_2 - \dot{\varphi}_1 + \dot{\varphi}_4 - \dot{\varphi}_3)$$

The last equation to solve the system is provided by the energy requirement. As it has been shown before, this corresponds to minimizing the function $P'(t) = U_1^2 + U_2^2 + U_3^2 + U_4^2$. This is exactly the same system of equations which was deduced to minimize the driving torques. In consequence, the solution is similar:

$$U_{1_{min}} = \frac{B'}{2} - \frac{C'}{4}$$

$$U_{2_{min}} = \frac{A'}{2} + \frac{C'}{4}$$

$$U_{3_{min}} = \frac{A'}{2} - \frac{C'}{4}$$

$$U_{4_{min}} = \frac{B'}{2} + \frac{C'}{4}$$

The following pictures correspond to simulations with given trajectories, considering the constants $C_u = 1{,}75\ \frac{N}{V}$; $C_v = 0{,}013\ N \cdot s$.

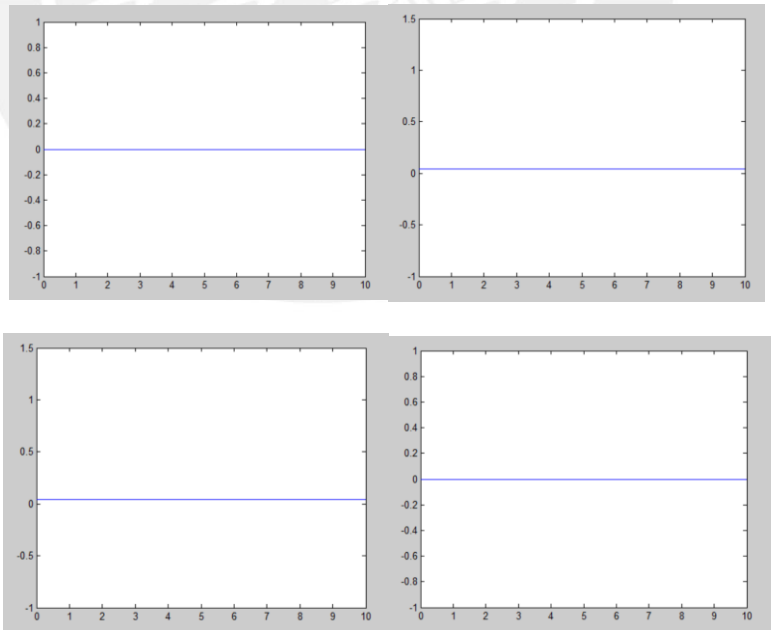

Figure 2.13. From top to bottom, left to right: Tension U_1, U_2, U_3 and U_4 for a trajectory $x = y = t$

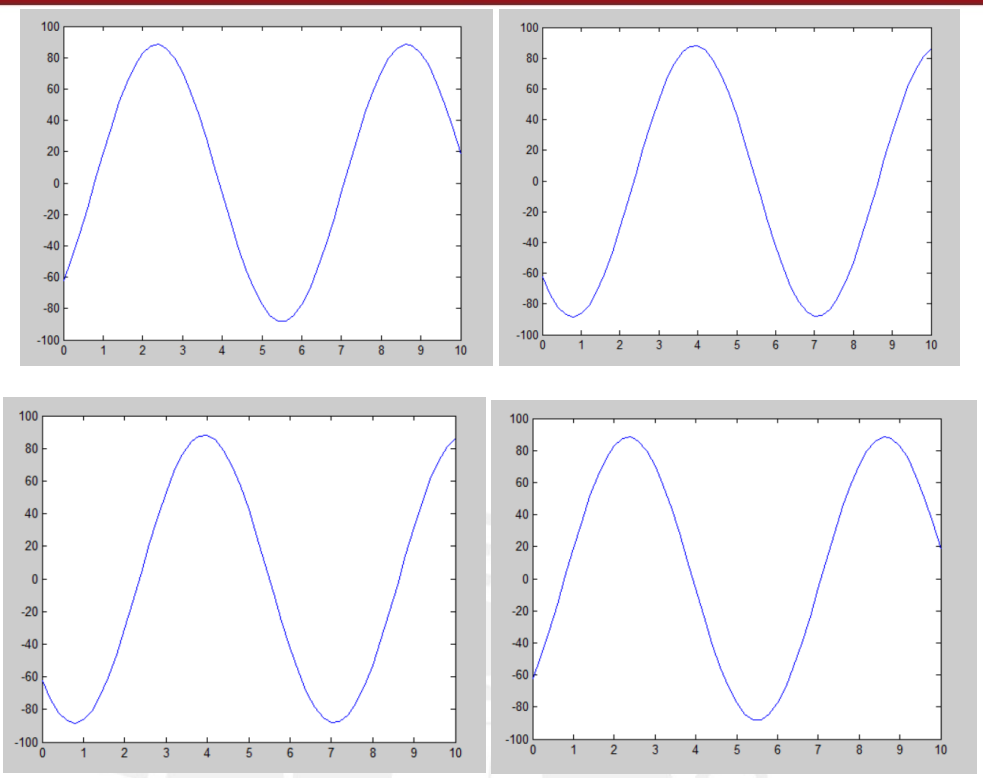

Figure 2.14. From top to bottom, left to right: Tension U_1, U_2, U_3 and U_4 for a trajectory $x = \cos(t)$, $y = \sin(t)$

2.6. Analysis of a Truck and Trailer System

Now that the equations of the robot with Mecanum wheels are completely known, it is of further interest of the research to evaluate systems on which a trailer is attached to the robot through a single rod. Four possible scenarios will then be analized:

- First scenario: Trailer with regular wheels, free angle between the rod and the trailer.
- Second scenario: Trailer with regular wheels, fixed angle of 90º between the rod and the trailer.
- Third scenario: Trailer with Mecanum wheels, free angle between the rod and the trailer.
- Fourth scenario: Trailer with Mecanum wheels, fixed angle of 90º between the rod and the trailer.

In all scenarios, a free angle between the rod and the robot is assumed.

Table 2.2. Robot-Trailer scenarios to be examined

	Conventional Wheel	Mecanum Wheel
$\theta \neq \beta$	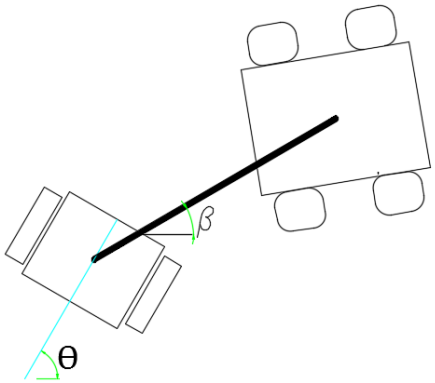	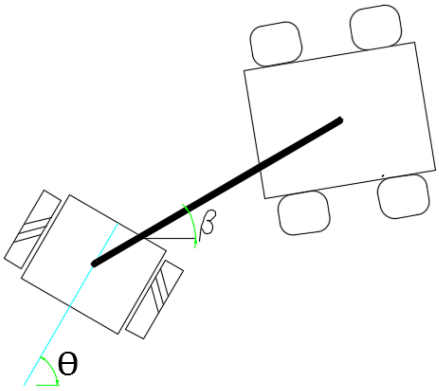
$\theta = \beta$	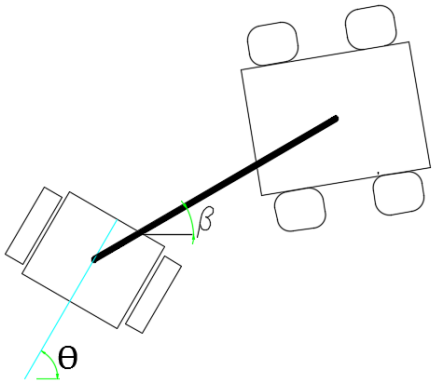	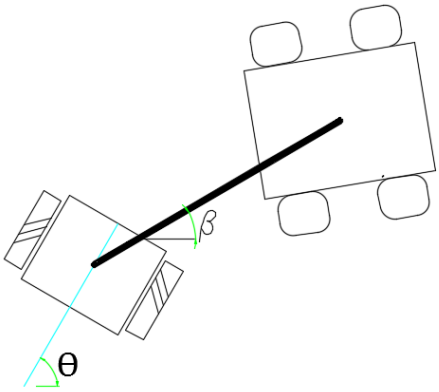

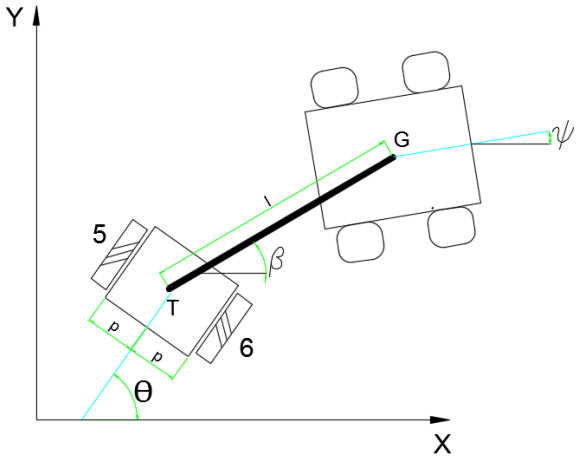

Figure 2.15. Scheme showing the robot-trailer system

a. First scenario

The truck consists of the Mecanum-wheeled robot, while the trailer consists on a two wheeled vehicle with radius R_t, which is connected to the truck via a rod between both centers of gravity.

The center of gravity will be assumed to be contained on the axis connecting both wheels. Thus, the coordinates for the center of the wheels 5 and 6 can be written as:

$$x_{O_5} = x_T - p\,\sin(\theta)$$

$$y_{O_5} = y_T + p\,\cos(\theta)$$

$$x_{O_6} = x_T + p\,\sin(\theta)$$

$$y_{O_6} = y_T - p\,\cos(\theta)$$

And the velocities:

$$\dot{x}_{O_5} = \dot{x}_T - p\dot{\theta}\,\cos(\theta)$$

$$\dot{y}_{O_5} = \dot{y}_T - p\dot{\theta}\,\sin(\theta)$$

$$\dot{x}_{O_6} = \dot{x}_T + p\dot{\theta}\,\cos(\theta)$$

$$\dot{y}_{O_6} = \dot{y}_T + p\dot{\theta}\,\sin(\theta)$$

These equations will be of further use. Now, analyzing the velocities on both ends of the rod:

$$\vec{v}_G = \vec{v}_T + \vec{\omega}_T \times \overrightarrow{TG}$$

Where ω_T is the angular velocity of the rod. This rod is considered to rotate freely and thus, has its own angular velocity $\dot{\beta}$.

The equation can be written using generalized coordinates x_T, y_T, θ, x_G and y_G.

$$(\dot{x}_G, \dot{y}_G) = (\dot{x}_T, \dot{y}_t) + (\dot{\beta}\vec{e}_z) \times \Big((l\cos(\beta))\vec{e}_x + (l\sin(\beta))\vec{e}_y\Big)$$

Two scalar equations can then be written:

$$\dot{x}_T = \dot{x}_G + \dot{\beta}\; l\sin(\beta)$$

$$\dot{y}_T = \dot{y}_G - \dot{\beta}\, l \cos(\beta)$$

The velocities of the wheel's center of mass are then rewritten as:

$$\dot{x}_{O_5} = \dot{x}_G + \dot{\beta} l \sin(\beta) - \dot{\theta} p \cos(\theta)$$

$$\dot{y}_{O_5} = \dot{y}_G - \dot{\beta} l \cos(\beta) - \dot{\theta} p \sin(\theta)$$

$$\dot{x}_{O_6} = \dot{x}_G + \dot{\beta} l \sin(\beta) + \dot{\theta} p \cos(\theta)$$

$$\dot{y}_{O_6} = \dot{y}_G - \dot{\beta} l \cos(\beta) + \dot{\theta} p \sin(\theta)$$

Now, the kinematic constrains of the system will be considered.

In this scenario, the wheels from the trailer are considered to be regular wheels.

Considering the constrain equations for a conventional wheel on a plane, as considered in Zimmermann *et al.*, the following constrain equations can be written.

$$\dot{x}_{O_i} \cos(\theta) + \dot{y}_{O_i} \sin(\theta) = R_t \dot{\varphi}_i$$

$$-\dot{x}_{O_i} \sin(\theta) + \dot{y}_{O_i} \cos(\theta) = 0$$

Where $i = 5{,}6$. Replacing the expressions as functions of the velocity of the robot's center of mass, three constrain equations can be deduced:

$$\dot{x}_G \cos(\theta) + \dot{y}_G \sin(\theta) - \dot{\beta} l \sin(\beta - \theta) - \dot{\theta} p = R_t \dot{\varphi}_5$$

$$\dot{x}_G \cos(\theta) + \dot{y}_G \sin(\theta) + \dot{\beta} l \sin(\beta - \theta) + \dot{\theta} p = R_t \dot{\varphi}_6$$

$$-\dot{x}_G \sin(\theta) + \dot{y}_G \cos(\theta) - \dot{\beta} l \cos(\beta - \theta) = 0$$

Together with the robot's constrain equation, the system can be described as follows:

$$\begin{bmatrix} \sin(\psi+\delta_1) & -\cos(\psi+\delta_1) & -l_1\cos(\delta_1)-d_1\sin(\delta_1) & 0 & 0 \\ \sin(\psi+\delta_2) & -\cos(\psi+\delta_2) & -l_1\cos(\delta_2)+d_2\sin(\delta_2) & 0 & 0 \\ \sin(\psi+\delta_3) & -\cos(\psi+\delta_3) & l_2\cos(\delta_3)-d_1\sin(\delta_3) & 0 & 0 \\ \sin(\psi+\delta_4) & -\cos(\psi+\delta_4) & l_2\cos(\delta_4)+d_2\sin(\delta_4) & 0 & 0 \\ \cos(\theta) & \sin(\theta) & 0 & l\sin(\beta-\theta) & -p \\ \cos(\theta) & \sin(\theta) & 0 & l\sin(\beta-\theta) & p \\ -\sin(\theta) & \cos(\theta) & 0 & -l\cos(\beta-\theta) & 0 \end{bmatrix} \begin{bmatrix} \dot{x_G} \\ \dot{y_G} \\ \dot{\psi} \\ \dot{\beta} \\ \dot{\theta} \end{bmatrix}$$

$$= \begin{bmatrix} R\dot{\varphi}_1\sin(\delta_1) \\ R\dot{\varphi}_2\sin(\delta_2) \\ R\dot{\varphi}_3\sin(\delta_3) \\ R\dot{\varphi}_4\sin(\delta_4) \\ R_t\dot{\varphi}_5 \\ R_t\dot{\varphi}_6 \\ 0 \end{bmatrix}$$

This shows clearly that there are eleven generalized coordinates and seven constrain equations, which means the system has four degrees of freedom. The system could be solved if four values of the angular velocities are given.

Nevertheless, $\dot{\varphi}_i$ must be carefully chosen in order to solve the system. For instance, if $\dot{\varphi}_1$, $\dot{\varphi}_2$, $\dot{\varphi}_3$ and $\dot{\varphi}_4$ are given in order to do so, the resultant matrix is singular. Hence, the system cannot be solved. At least one of the angular velocities from $\dot{\varphi}_1$ to $\dot{\varphi}_4$ must remain unknown in order not to over-constrain the system, more specifically, the robot's movement.

The singularity arises from the first four equations. This is physically explained by the fact that the first three coordinates $\dot{x_G}$, $\dot{y_G}$, $\dot{\psi}$ are determined just by $\dot{\varphi}_1$, $\dot{\varphi}_2$ and $\dot{\varphi}_3$. As the robot's movement is fully defined by the movement of three of its wheels, adding a fourth angular velocity would over-constrain the system. For this reason, an angular velocity other than $\dot{\varphi}_4$ should be chosen in order to solve the equations.

b. Second Scenario

In this scenario, the trailer and the rod are considered to have a fixed angle for the entire motion. Thus, both bodies have now the same angular velocity, this is: $\dot{\beta} = \dot{\theta}$

Considering this fact, the velocity for the trailer center of mass can be written as:

$$\dot{x}_T = \dot{x}_G + \dot{\theta}\, l\sin(\theta)$$

$$\dot{y}_T = \dot{y}_G - \dot{\theta}\, l \cos(\theta)$$

As last step, the velocities are expressed as functions of the velocity of the robot's center of mass:

$$\dot{x}_{O_5} = \dot{x}_G + \dot{\theta}(l \sin(\theta) - p \cos(\theta))$$

$$\dot{y}_{O_5} = \dot{y}_G - \dot{\theta}(l \cos(\theta) + p \sin(\theta))$$

$$\dot{x}_{O_6} = \dot{x}_G + \dot{\theta}(l \sin(\theta) + p \cos(\theta))$$

$$\dot{y}_{O_6} = \dot{y}_G - \dot{\theta}(l \cos(\theta) - p \sin(\theta))$$

Similarly to the first scenario, three constrain equations can be written from these formulas:

$$\dot{x}_G \cos(\theta) + \dot{y}_G \sin(\theta) - \dot{\theta} p = R_t \dot{\varphi}_5$$

$$\dot{x}_G \cos(\theta) + \dot{y}_G \sin(\theta) + \dot{\theta} p = R_t \dot{\varphi}_6$$

$$-\dot{x}_G \sin(\theta) + \dot{y}_G \cos(\theta) - \dot{\theta} l = 0$$

The complete system of equations, including those of the robot, are represented in the following matrix:

$$\begin{bmatrix} \sin(\psi + \delta_1) & -\cos(\psi + \delta_1) & -l_1 \cos(\delta_1) - d_1 \sin(\delta_1) & 0 \\ \sin(\psi + \delta_2) & -\cos(\psi + \delta_2) & -l_1 \cos(\delta_2) + d_2 \sin(\delta_2) & 0 \\ \sin(\psi + \delta_3) & -\cos(\psi + \delta_3) & l_2 \cos(\delta_3) - d_1 \sin(\delta_3) & 0 \\ \sin(\psi + \delta_4) & -\cos(\psi + \delta_4) & l_2 \cos(\delta_4) + d_2 \sin(\delta_4) & 0 \\ \cos(\theta) & \sin(\theta) & 0 & -p \\ \cos(\theta) & \sin(\theta) & 0 & p \\ -\sin(\theta) & \cos(\theta) & 0 & l \end{bmatrix} \begin{bmatrix} \dot{x}_G \\ \dot{y}_G \\ \dot{\psi} \\ \dot{\theta} \end{bmatrix} = \begin{bmatrix} R\dot{\varphi}_1 \sin(\delta_1) \\ R\dot{\varphi}_2 \sin(\delta_2) \\ R\dot{\varphi}_3 \sin(\delta_3) \\ R\dot{\varphi}_4 \sin(\delta_4) \\ R_t \dot{\varphi}_5 \\ R_t \dot{\varphi}_6 \\ 0 \end{bmatrix}$$

There are seven constrain equations against ten generalized coordinates, which gives the system 3 degrees of freedom. These means that $\dot{\varphi}_1$ through $\dot{\varphi}_3$ can still be chosen in order to know the rest of variables. To do so, the equations must be rearranged as:

$$\begin{bmatrix} \sin(\psi+\delta_1) & -\cos(\psi+\delta_1) & -l_1\cos(\delta_1)-d_1\sin(\delta_1) & 0 & 0 & 0 & 0 \\ \sin(\psi+\delta_2) & -\cos(\psi+\delta_2) & -l_1\cos(\delta_2)+d_2\sin(\delta_2) & 0 & 0 & 0 & 0 \\ \sin(\psi+\delta_3) & -\cos(\psi+\delta_3) & l_2\cos(\delta_3)-d_1\sin(\delta_3) & 0 & 0 & 0 & 0 \\ \sin(\psi+\delta_4) & -\cos(\psi+\delta_4) & l_2\cos(\delta_4)+d_2\sin(\delta_4) & 0 & -R\sin(\delta_4) & 0 & 0 \\ \cos(\theta) & \sin(\theta) & 0 & -p & 0 & -R_t & 0 \\ \cos(\theta) & \sin(\theta) & 0 & p & 0 & 0 & -R_t \\ -\sin(\theta) & \cos(\theta) & 0 & l & 0 & 0 & 0 \end{bmatrix} \begin{bmatrix} \dot{x_G} \\ \dot{y_G} \\ \dot{\psi} \\ \dot{\theta} \\ \dot{\varphi_4} \\ \dot{\varphi_5} \\ \dot{\varphi_6} \end{bmatrix}$$

$$= \begin{bmatrix} R\dot{\varphi_1}\sin(\delta_1) \\ R\dot{\varphi_2}\sin(\delta_2) \\ R\dot{\varphi_3}\sin(\delta_3) \\ 0 \\ 0 \\ 0 \\ 0 \end{bmatrix}$$

Introducing the following velocities $\dot{\varphi_1} = \dot{\varphi_2} = \dot{\varphi_3} = 0{,}5t$, the following results are achieved for the trajectory and the angular velocity of the driven wheels:

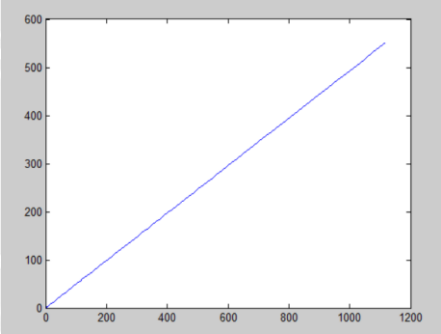

Figure 2.16. Trajectory of the robot's center of mass

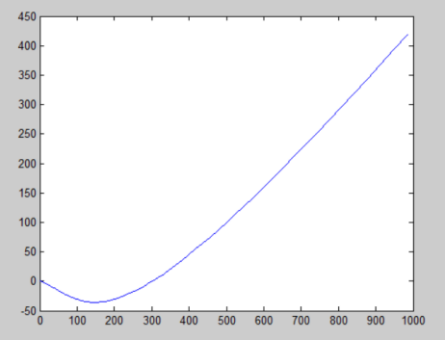

Figure 2.17. Trajectory of the trailer's center of mass

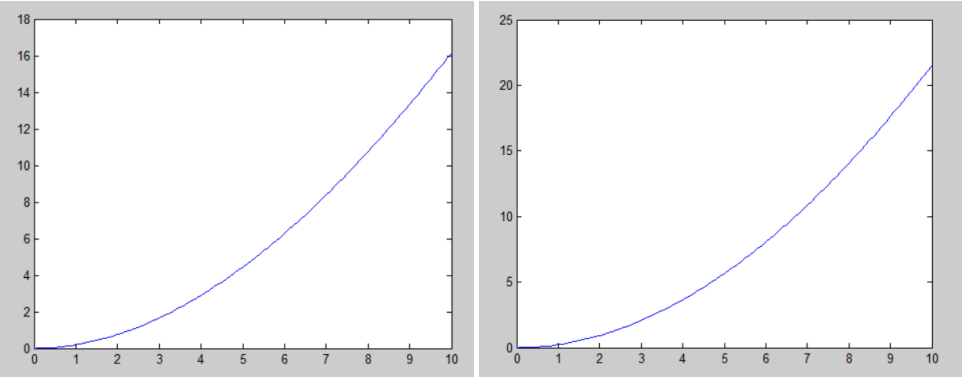

Figure 2.18. Angular velocities of wheels 5 (left) and 6 (right).

a. Third scenario

In this scenario, Mecanum wheels are considered for the trailer, as well as a non-fixed angle between the trailer and the connection rod. As with the second scenario, two constrain equations can be written from these conditions:

$$\dot{x}_{O_5}\sin(\theta+\delta_5)-\dot{y}_{O_5}\cos(\theta+\delta_5)+\dot{\beta}l\cos(\beta-\theta-\delta_5)-\dot{\theta}p\sin(\delta_5)=R\dot{\varphi}_5\sin(\delta_5)$$

$$\dot{x}_{O_6}\sin(\theta+\delta_6)-\dot{y}_{O_6}\cos(\theta+\delta_6)+\dot{\beta}l\cos(\beta-\theta-\delta_5)+\dot{\theta}p\cos(\delta_5)=R\dot{\varphi}_6\sin(\delta_6)$$

The system can be described then by the following equations:

$$\begin{bmatrix}\sin(\psi+\delta_1) & -\cos(\psi+\delta_1) & -l_1\cos(\delta_1)-d_1\sin(\delta_1) & 0 & 0\\ \sin(\psi+\delta_2) & -\cos(\psi+\delta_2) & -l_1\cos(\delta_2)+d_2\sin(\delta_2) & 0 & 0\\ \sin(\psi+\delta_3) & -\cos(\psi+\delta_3) & l_2\cos(\delta_3)-d_1\sin(\delta_3) & 0 & 0\\ \sin(\psi+\delta_4) & -\cos(\psi+\delta_4) & l_2\cos(\delta_4)+d_2\sin(\delta_4) & 0 & 0\\ \sin(\theta+\delta_5) & -\cos(\theta+\delta_5) & 0 & l\cos(\beta-\theta-\delta_5) & l\cos(\delta_5)-p\sin(\delta_5)\\ \sin(\theta+\delta_6) & -\cos(\theta+\delta_6) & 0 & l\cos(\beta-\theta-\delta_5) & l\cos(\delta_6)+p\sin(\delta_6)\end{bmatrix}\begin{bmatrix}\dot{x}_G\\ \dot{y}_G\\ \dot{\psi}\\ \dot{\beta}\\ \dot{\theta}\end{bmatrix}$$

$$=\begin{bmatrix}R\dot{\varphi}_1\sin(\delta_1)\\ R\dot{\varphi}_2\sin(\delta_2)\\ R\dot{\varphi}_3\sin(\delta_3)\\ R\dot{\varphi}_4\sin(\delta_4)\\ R_t\dot{\varphi}_5\sin(\delta_5)\\ R_t\dot{\varphi}_6\sin(\delta_6)\end{bmatrix}$$

With six constrain equations and eleven generalized coordinates, the system has now five degrees of freedom. Moreover, as with the first scenario, at least one angular velocity between $\dot{\varphi}_1$ and $\dot{\varphi}_4$ must remain unknown in order to properly solve the system of equations.

b. Fourth scenario

This scenario, as well as the second one, considers now a fixed angle between the trailer and the rod, which implies that both bodies share the same angular velocity.

Replacing the expressions for $\dot{x}_{O_5}$, $\dot{y}_{O_5}$, $\dot{x}_{O_6}$ and $\dot{y}_{O_6}$ as functions of $\dot{x}_G$ and $\dot{y}_G$ obtained in the analysis of the second scenario in the constrain equations for Mecanum wheels, the constrain equations for this system are deduced:

$$\dot{x}_{O_5}\sin(\theta+\delta_5)-\dot{y}_{O_5}\cos(\theta+\delta_5)+\dot{\theta}(l\cos(\delta_5)-p\sin(\delta_5))=R\dot{\varphi}_5\sin(\delta_5)$$

$$\dot{x}_{O_6}\sin(\theta+\delta_6)-\dot{y}_{O_6}\cos(\theta+\delta_6)+\dot{\theta}(l\cos(\delta_6)+p\sin(\delta_6))=R\dot{\varphi}_6\sin(\delta_6)$$

Combining these new equations with the robot's constrains, the new system of equations can be written as:

$$\begin{bmatrix}\sin(\psi+\delta_1) & -\cos(\psi+\delta_1) & -l_1\cos(\delta_1)-d_1\sin(\delta_1) & 0\\ \sin(\psi+\delta_2) & -\cos(\psi+\delta_2) & -l_1\cos(\delta_2)+d_2\sin(\delta_2) & 0\\ \sin(\psi+\delta_3) & -\cos(\psi+\delta_3) & l_2\cos(\delta_3)-d_1\sin(\delta_3) & 0\\ \sin(\psi+\delta_4) & -\cos(\psi+\delta_4) & l_2\cos(\delta_4)+d_2\sin(\delta_4) & 0\\ \sin(\theta+\delta_5) & -\cos(\theta+\delta_5) & 0 & l\cos(\delta_5)-p\sin(\delta_5)\\ \sin(\theta+\delta_6) & -\cos(\theta+\delta_6) & 0 & l\cos(\delta_6)+p\sin(\delta_6)\end{bmatrix}\begin{bmatrix}\dot{x}_G\\ \dot{y}_G\\ \dot{\psi}\\ \dot{\theta}\end{bmatrix}$$
$$=\begin{bmatrix}R\dot{\varphi}_1\sin(\delta_1)\\ R\dot{\varphi}_2\sin(\delta_2)\\ R\dot{\varphi}_3\sin(\delta_3)\\ R\dot{\varphi}_4\sin(\delta_4)\\ R_t\dot{\varphi}_5\sin(\delta_5)\\ R_t\dot{\varphi}_6\sin(\delta_6)\end{bmatrix}$$

There are 6 equations and 10 generalized coordinates, which gives the system 4 degrees of freedom. The system could be solved if four values of the angular velocities are given. It should be noted that here, as it happened with the first and third scenarios, the angular velocities chosen as known must be carefully evaluated.

For example, choosing $\dot{\varphi}_1$, $\dot{\varphi}_2$,$\dot{\varphi}_3$ and $\dot{\varphi}_6$ as the known angular velocities, the following results are achieved:

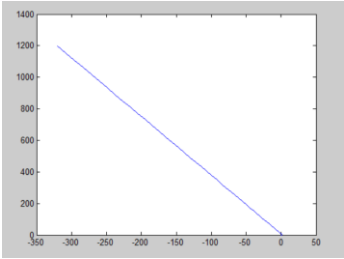

Figure 2.19. Trajectory of the robot's center of mass

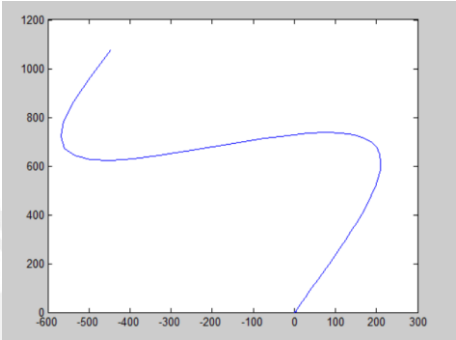

Figure 2.20. Trajectory of the trailer's center of mass

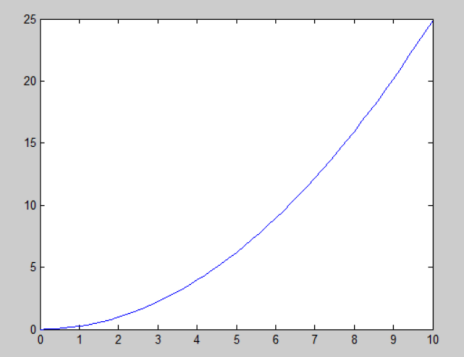

Figure 2.21. Angular velocity $\dot{\varphi}_4$ from the fourth wheel of the robot

CHAPTER THREE

DESIGN AND CONSTRUCTION OF THE TRAILER

Besides the theoretical models developed in the previous chapters, another of the objectives of this thesis is to design and build a trailer, which is to be attached to the robot. The main objective of this construction is to be able to compare the mathematical models obtained in the previous chapter to the physical results.

The trailer was design with the overall perspective of it being as simple as possible. Therefore, almost all parts were selected from the local market and only few of them were manufactured. This procedure allowed the simplicity of the design as well as the rapid construction of it.

3.1. General requirements

Though of simple construction, the trailer's design must fulfill some general requirements, which are listed below.

a) Dimensions: the trailer must have similar dimensions as the ones of the robot, both in height and width. A general tolerance of $\pm 15\ mm$ was placed as constrain in order to achieve this goal. The length has no restrictions.
b) Number of wheels: the trailer must use two Mecanum wheels, placed on the same axis with no shaft connecting them (each wheel can turn independently from each other). No power on the wheels is to be used.
c) Connection between robot and trailer: this must be achieved using a rod which length is variable. Additionally, a free rotation joint around an axis perpendicular to the robot's motion was considered for the connection on the robot, while a free rotation joint as well as a fixed joint were considered for the trailer.

3.2. Existing parts

The only existing part, which played an important role in the general design of the trailer, was the Mecanum wheel, which was manufactured at the Technische Universität Ilmenau. The main advantage of this wheel, when compared to the wheels on the robot, is that the angle of the rollers are not fixed. This is achieved via a gear mechanism in the interior of the wheel.

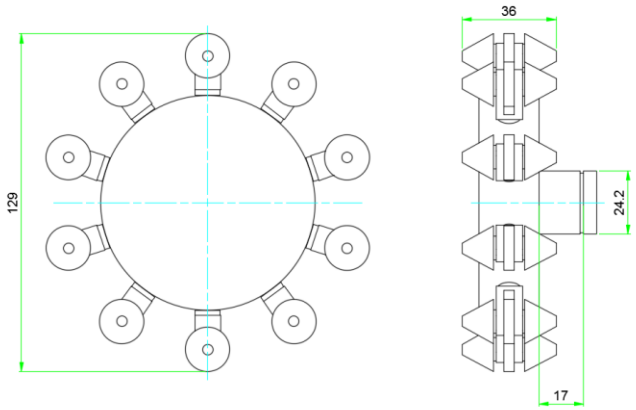

Fig 3.1. General dimensions of wheel manufactured at TU Ilmenau. The rollers on this representation have an angle $\delta = 0°$

Three main aspects of the wheel were taken into consideration for the trailer's design:

a) External diameter of $129\ mm$. The lowest part must be at the same level of that of the robot's wheels, which have a diameter of $100\ mm$.
b) Available length on the shaft. The length of the shaft that was proper to machine was $17\ mm$, as the rest of the shaft is used to configure the rollers' angles.
c) Shaft diameter of $24{,}2\ mm$.

3.3. Design of the structure

To mount the wheels on to the trailer, a support structure had to be designed. This had to be light, so as to reduce the inertia of the trailer, but also stable and able to support the wheels and the joint properly. Many elementary alternatives were devised, which are shown on figures 3.2 to 3.5.

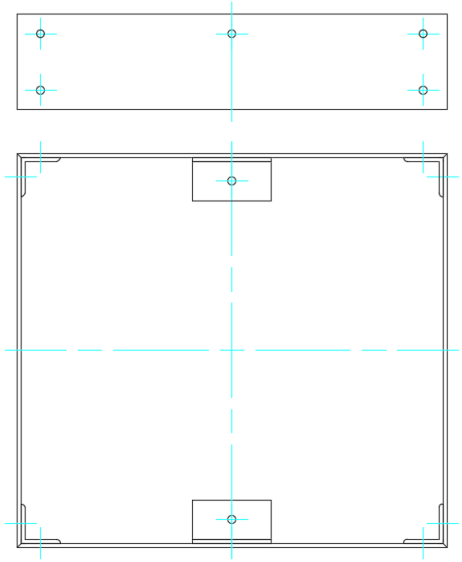

Fig. 3.2. Structure based on thin metal plates, assembled using L-shape profiles and screws (front and back views)

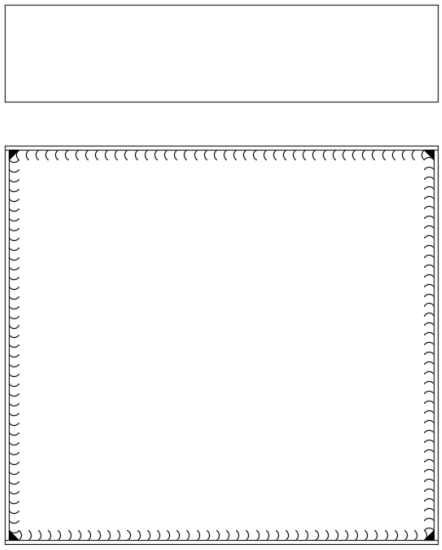

Fig. 3.3. Structure based on thin welded metal plates

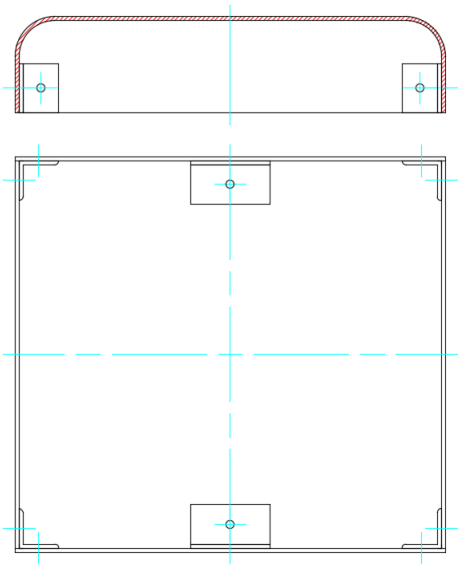

Fig 3.4. Structure based on folded metal plates joined with L-shaped profiles and screws

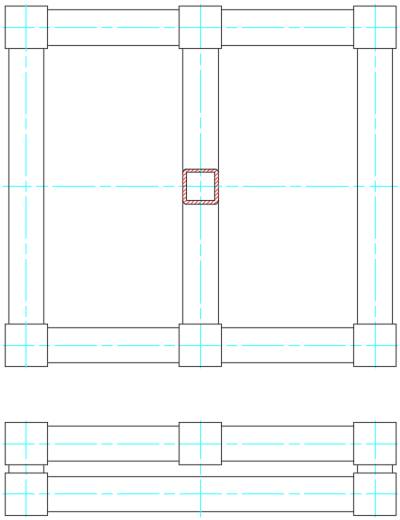

Fig. 3.5. Structure based on Square-section aluminum rods with connectors

As the main objective of the structure is to provide support for the wheels and the joint, while at the same time being light as well as providing an uncomplicated assemble, a structure based on aluminum rods was chosen. Nevertheless, the structure was further modified due to space and configuration reasons. The final structure achieved can be seen in figure 3.6.

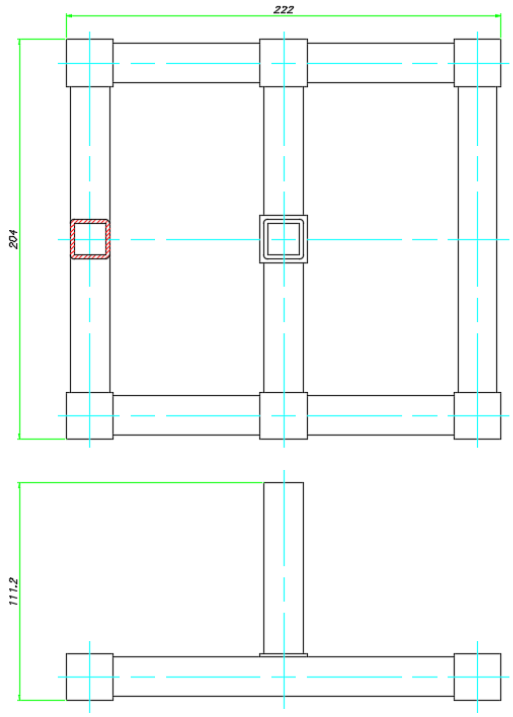

Fig. 3.6. Structure's final design

3.4. Design of the joints

The connection between robot and trailer requires an adequate design of the joint mechanisms, so that no interference with any other part, for instance, the wheels, is encountered.

As for the joint on the robot, it was decided that this joint should allow free movement around an axis perpendicular to the motion. On the other hand, the trailer should have two alternatives: one which allows a movement similar to that on the robot as well as one which fixes the angle between the rod and the trailer on $90°$. Additionally, these joint alternatives should be interchangeable with each other.

A handful of options were considered for all the possible scenarios, which are presented on figures 3.7 to 3.10.

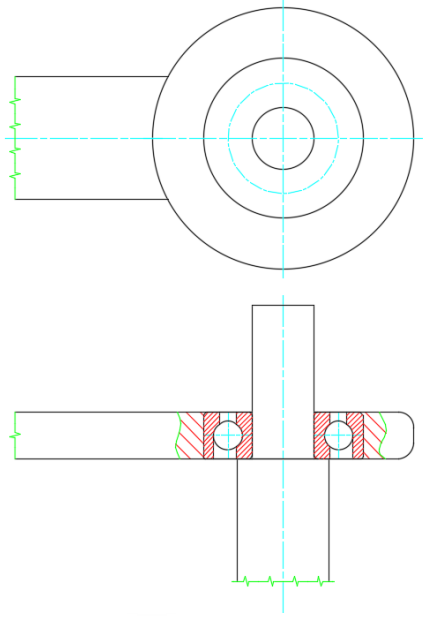

Figure 4.7. Joint system using a roller bearing to provide the tangential motion

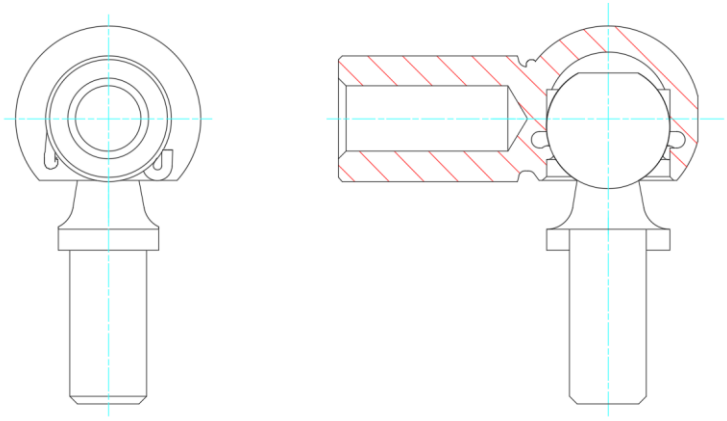

Fig 4.8. Connection using a spherical joint (model taken from MBO-Osswald)

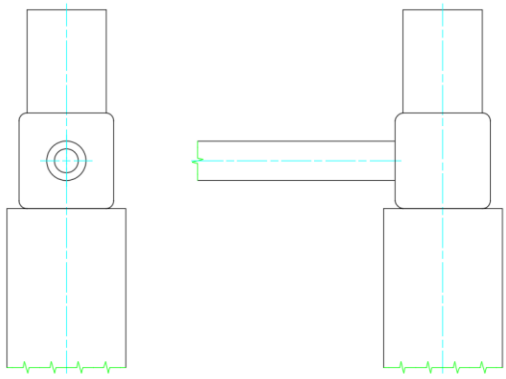

Fig. 4.9. Joint system using an eyebolt to provide the tangential motion

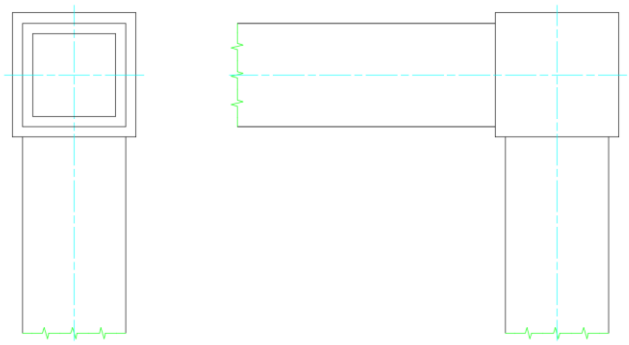

Fig. 4.10. Rigid joint using a 90° elbow connection

Considering that the trailer would only have two wheels on the same axis, any possibility which could lead to potential motion around such axis was ruled out due to stability reasons. Moreover, as both the fixed-angle alternative as well as the free-rotation one shall be interchangeable with each other, the joints depicted in figures 3.9 and 3.10 were chosen for the design.

Similarly to the case of the structure, these alternatives were further modified during the design phase until the configurations shown in figures 3.11 and 3.12 were achieved.

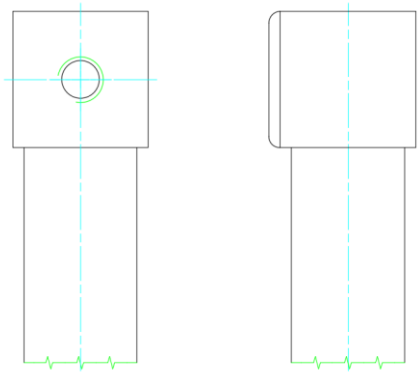

Fig. 3.11. Fixed connection final design

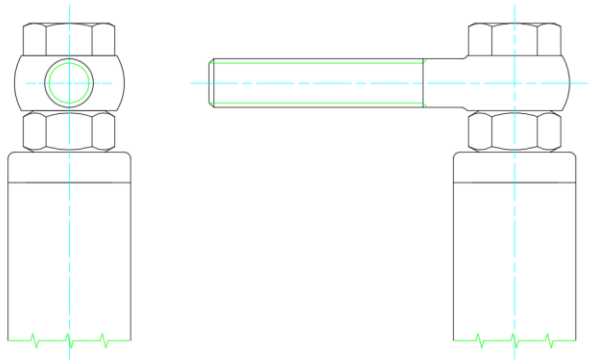

Fig. 3.12. Joint final design

4.5. Wheel support design

As it has been noted on section 3.2, the wheels which were to be used on the trailer design had already been built. To assembly them properly to the trailer, a support had to be design to meet the specific geometric requirements of both the trailer and the wheel itself.

As the shaft where the wheel has a diameter of $24{,}2\ mm$, there is no standard roller bearing which could be suitable. Thus, a compensating ring with a standard outer diameter had to be manufactured in order to properly assembly the wheel to the structure. The roller bearing which was chosen has an inner diameter of $30\ mm$, as the compensating ring had to have a proper thickness in order not to be damaged during operation.

Additionally, the length of the shaft which could be used to support the wheel was $17\ mm$, as a longer dimension would interfere with the rollers mechanism to change its angle with respect to the wheel axis.

With these ground requirements, the support for the wheel was designed. It consists of five parts: (1) the roller bearing, (2) a locking ring, (3) the compensating ring, (4) the housing for the bearing and the ring and (5) the cover for the housing. All the parts, with exception of the roller bearing and the locking ring, were manufactured at TU Ilmenau.

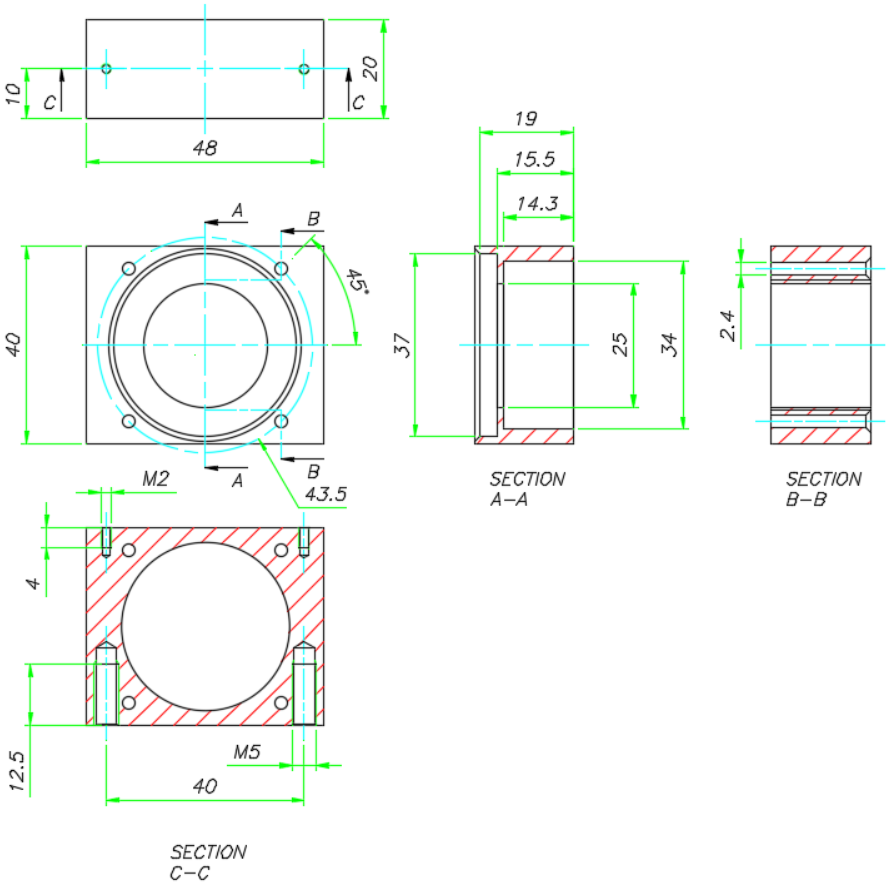

Fig 3.13. Main views and sectionsof the housing for the roller bearing and wheel shaft

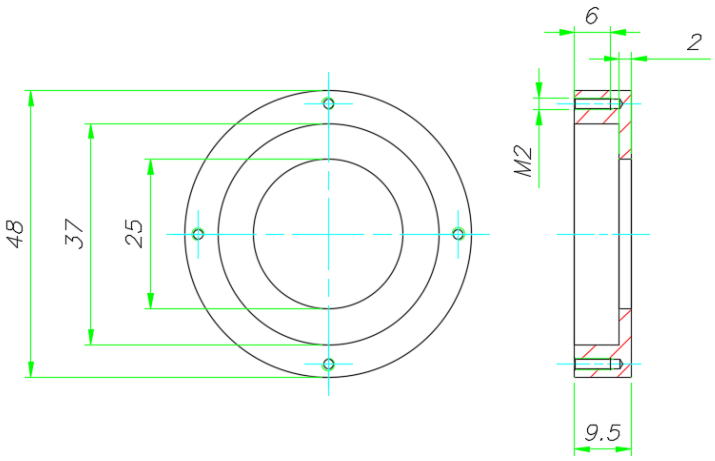

Fig. 3.14. Main view and section of the housing cover

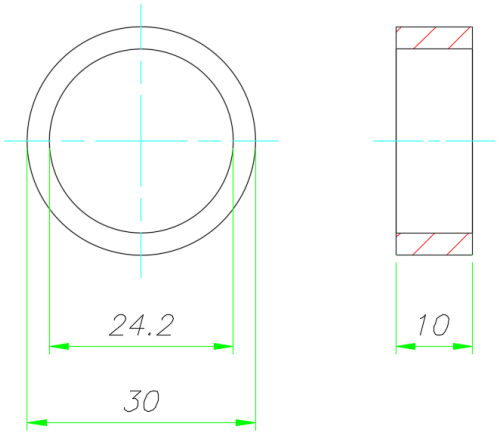

Fig. 3.15. Main views of the compensating ring

HK 3012

Dimensions

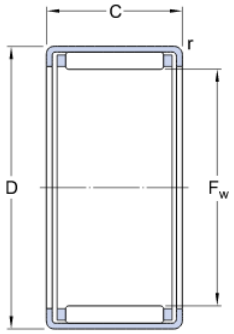

F_w		30	mm
D		37	mm
C		12	mm
r	min.	0.8	mm

Fig. 3.16. Selected roller bearing (image taken from SKF at www.skf.com/de/)

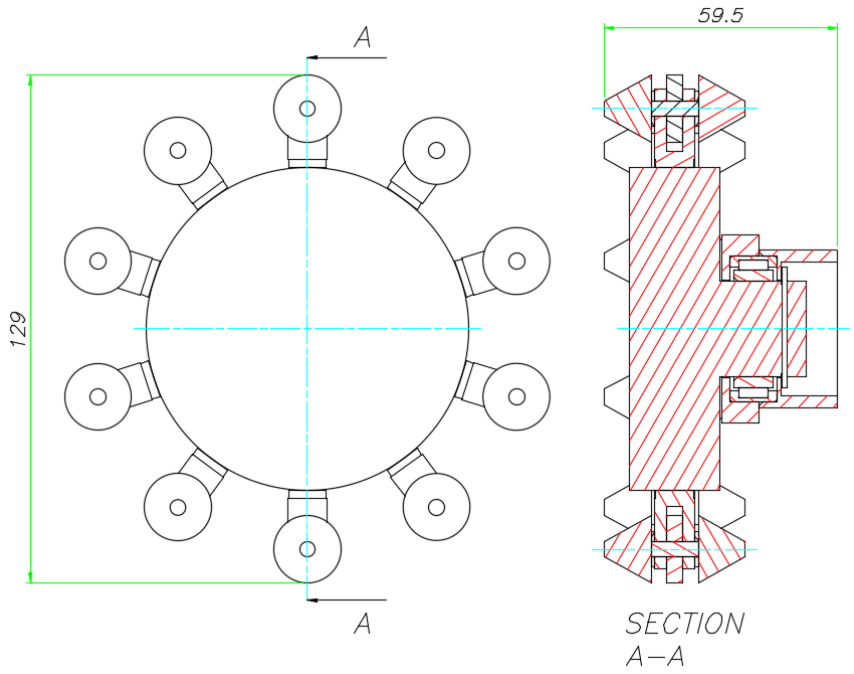

Fig. 3.17. Main view and section view of the whole assembly

3.6. Additional parts

Besides the components which were required and design in the previous points, the following pieces were either buy or designed:

a) A twist-and-lock bar (usually used to support shower curtains), in order to connect both robot and trailer and to make the length of the connection variable.
b) A base plate for the robot, in order to ensure the stability on the joint.
c) Various screws, nuts and threaded connectors to assembly the parts mentioned in the above sections.
d) Yellow flexible plates to cover the structure and give aesthetics to the assembly.

CHAPTER FOUR

FULL ASSEMBLY AND DESIGN VERIFICATION

All the elements mentioned in the previous chapter were either bought or manufactured at the workshops of the TU Ilmenau. Photos of the assembled trailer can be seen in figures 4.1 to 4.5.

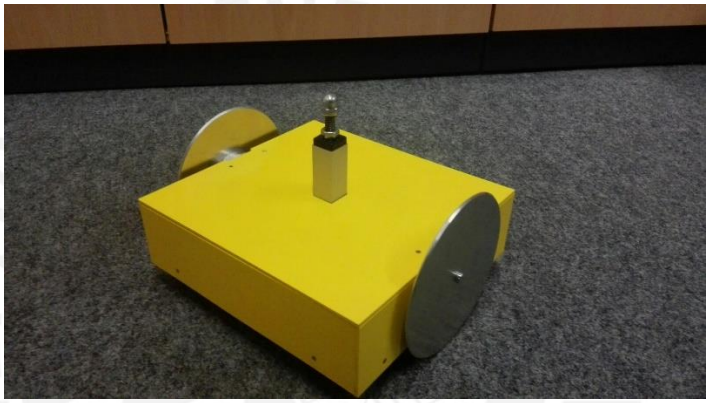

Figure 4.1. Assembled trailer without the Mecanum wheels.

Figure 4.2. Back side of the trailer and detail of the structure.

Figure 4.3. Roller bearing housing manufactured at TU Ilmenau

The trailer, as was seen on the pictures above, has conventional wheels attached to each side. The Mecanum wheel that was manufactured at TU Ilmenau can be seen on picture 4.4.

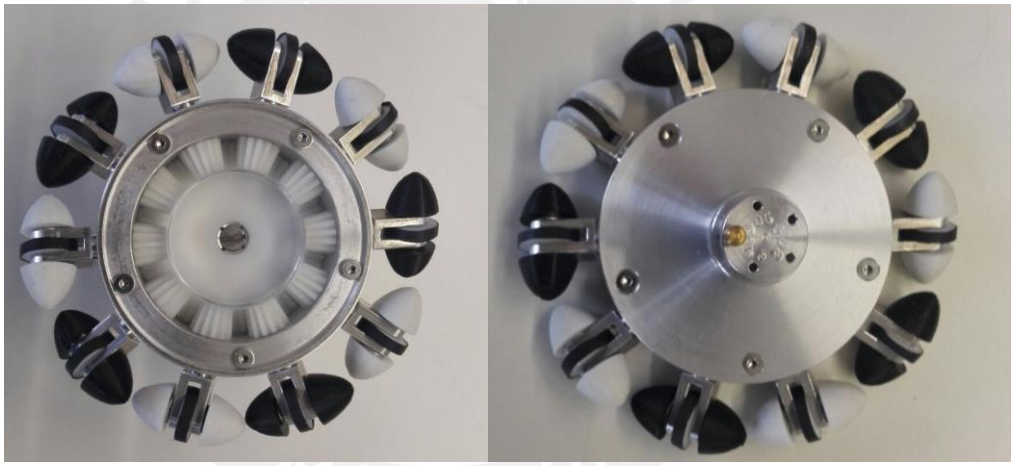

Fig. 4.4. Front (right) and back (left) views of the Mecanum wheel manufactured at TU Ilmenau.

As it can be seen on the figure above, the gear mechanism inside the wheel allow the user to change the relative angle between the wheel and the rollers.

The trailer can be used with both conventional wheels or Mecanum wheels. Figures 4.5 and 4.6 show the Mecanum wheels manufactured at TU Ilmenau attached to the trailer.

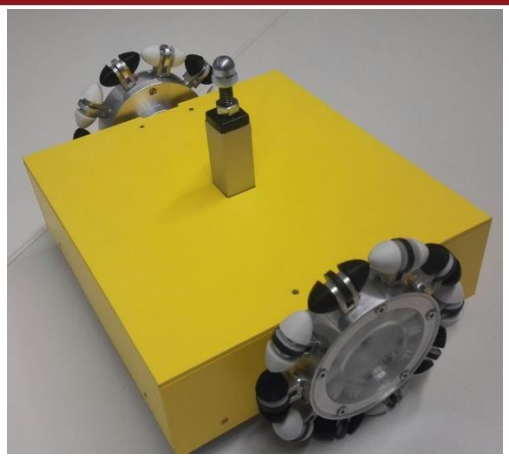

Figure 4.5. Manufactured Mecanum wheels mounted on the trailer.

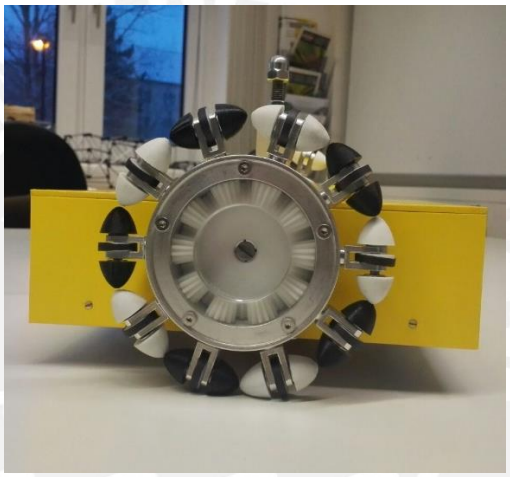

Figure 4.6. Side view of the trailer assembly

On figure 4.7 both can be observed: the conventional wheel mounted on the trailer, the Mecanum wheel on one side.

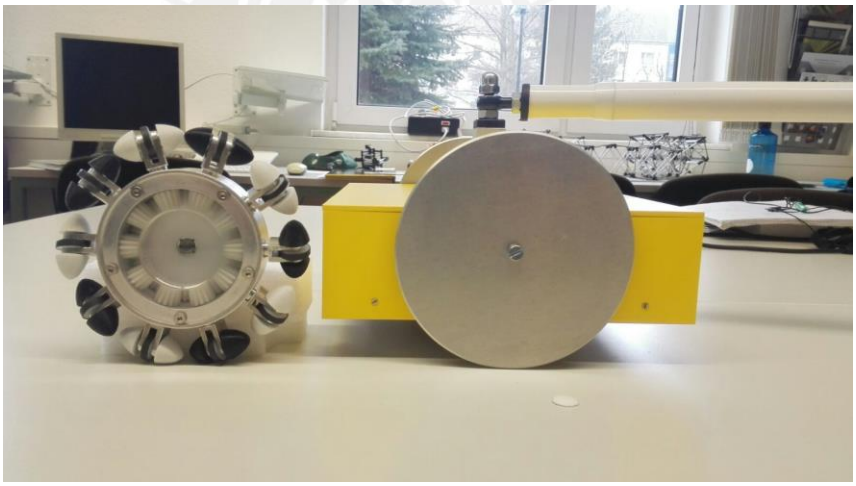

Fig. 4.7. Mecanum wheel and conventional wheel.

The robot used to drive the trailer was the 100 mm Mecanum Wheel robot kit 100111 – Nexus Robot, property of the department of technical mechanics at the TU Ilmenau. It has four independent motors on each wheel, which allow the motion of the system to be controlled remotely.

Fig. 4.8. Nexus robot before being attached to the trailer

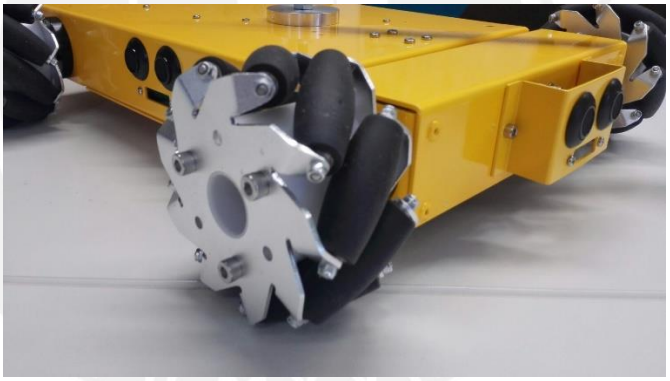

Fig. 4.9. Detail of the Mecanum wheel on the Nexus robot

The robot's structure was further modified in order to assembly the joint. A circular metal base was connected to the top plate of the robot using screws. The base itself has a M8 screwed through hole to connect the large screw in which the joint was assembled. A detail of the connection can be seen on figure 4.10.

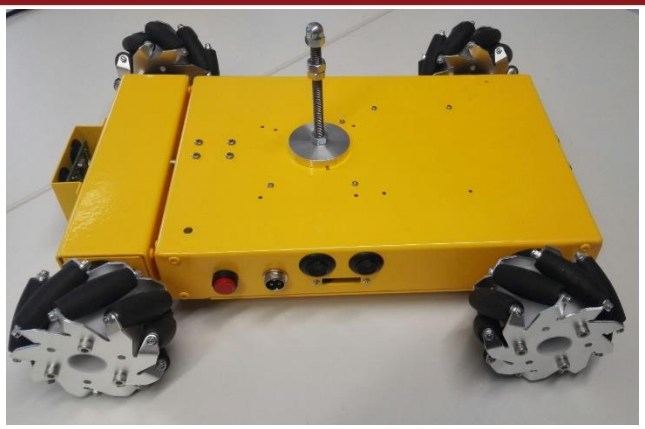

Fig. 4.10. Circular metal base, screw and nut on the robot's top plate

After the full assembly was made, the model was tested for functionality and mobility, both with conventional and Mecanum wheels. Figures 4.11 and 4.12 show the different views of the final assembly.

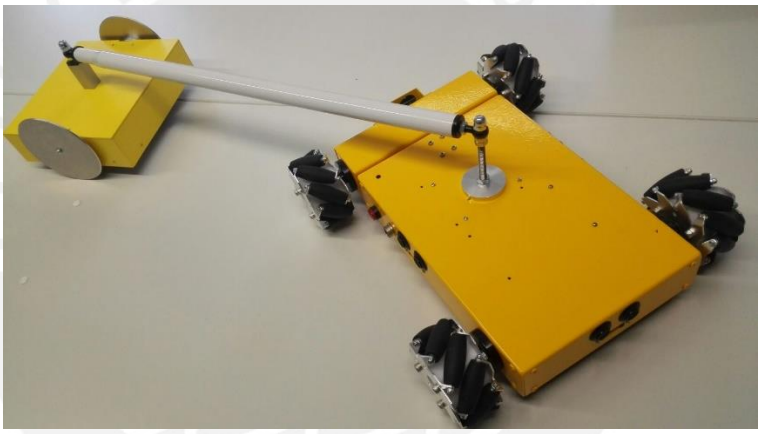

Fig. 4.11. View of the final assembly using mobile joints on both robot and trailer

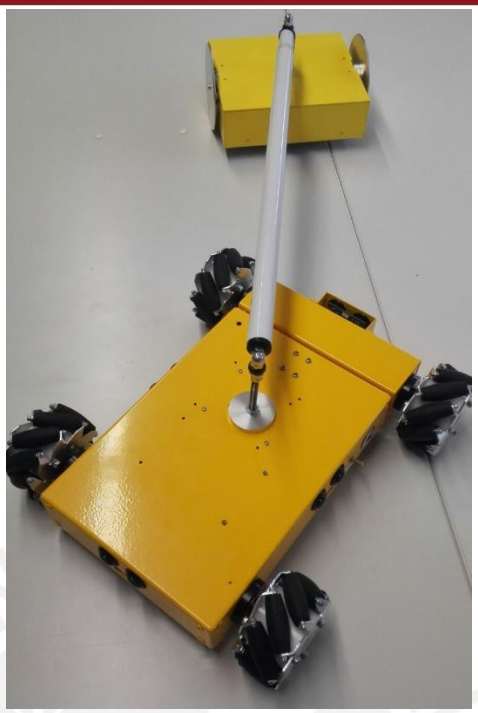

Fig. 4.12. The telescopic pole, which connects robot and trailer, allow the connecting distance to vary between the two bodies of the system

CONCLUSIONS AND FUTURE WORK

A mathematical model was developed in order to calculate and simulate the trajectories of the center of mass that a four-Mecanum-wheeled robot would follow given various parameters, which can be controlled. Through the deduction of the equations, it could be verified that it could be modelled as a three-degree-of-freedom body.

At a first stage, the model just considered the kinematic variables on the system, and so the parameters that were given to the model were the angular velocities on three wheels for the direct kinematics approach. The inverse kinematics could also be solved for a defined trajectory.

It is worth mentioning that, in this stage, an exact solution to the differential equations was given without the use of an approximation method, such as the use of the pseudo-inverse matrix. Nevertheless, as stated by Muir and Neuman, the actuators present on the robot are sufficient to provide motion on the three degrees of freedom on the plane, but can lead to actuator conflict. The fact that only three angular velocities are needed to solve the equations clearly shows that the motion on the fourth wheel could be in conflict with any, if not all, the remaining motors. This can be also observed in a further chapter with a robot-trailer system.

At a second stage, Lagrange equations with multipliers were used to deduce the kinetic system of differential equations of motion. Using this kind of equations allows the deduction of the latter for non-holonomic systems. Once they were calculated, the parameters given to the simulation were the driving torques on each wheel to solve the system of equations.

Furthermore, an optimization condition was given as an additional equation to calculate the optimal driving torque on each wheel for any given trajectory. The linear dependence proposed by Gorinevsky was used to stablish a relation between the torque and the voltage on each driving motor. No loses were assumed due to friction, heat generation or eddy current. Thus, all the power generated by the motor was assumed to be transferred to the robot.

The power on each driving motor was assumed to be proportional to the square of the voltage applied to it. Thus, the total power of the motor was proportional to the sum of the powers of each individual motor. The relation between the torque and the voltage

allows to assume that this total power should also be proportional to the driving torques provided by each motor.

In order to minimize the total power, a dependency had to be stablished between three driving torques and the remaining one. This was possible thanks to the three equations of motion deduced from the Lagrange equations. Once a relation was stablished, the power equation could be written in terms of just one driving torque. This equation was derived with respect to the latter, allowing writing the fourth torque in terms of $x(t), y(t)$ and their time derivatives. Hence, the remaining torques were calculated once one of them was known.

A robot and trailer system was also modeled only at a kinematic level, showing the degrees of freedom for each of the four scenarios that were considered for such system. In this scenarios, it was also evident the fact that, even though the system has more degrees of freedom and thus, more variables are required to solve the system of equations, only three angular velocities corresponding to the robot kinematics are to be specified.

The entire modelling was done for a general robot with an unsymmetrical center of mass and a general angle between the rollers and the main body axes. As for the trailer, the center of gravity was considered to be in the same axis as the wheels.

The results obtained in the simulation must be further verified with real data obtained from the models that were described in chapter four. Once verified, optimal operation routines for a determined task could be programmed for the robot to optimize the energy used in each operation.

Furthermore, the dynamics of the robot-trailer system must be calculated in order to obtain the differential equations of motion for the entire system. The Lagrange equations with multipliers method is also valid for this model, as the system is still non-holonomic.

REFERENCES

[1] De Luca, A. and Oriolo, G. Modeling and Control of Nonholonomic Mechanical Systems. Dipartamento di Informatica e Sistemistica. Università degli Studi di Roma "La Sapienza". Rome, Italy.

[2] Sarkar, N.; Yun, X. and Kumar, V. Control of Mechanical Systems with Rolling Constraints: Application to Dynamic Control of Mobile Robots. General Robotics and Active Sensory Perception Laboratory. University of Pennsylvania. Philadelphia, United States of America.

[3] Tilbury, D.; Murray, R. and Sastry, S. Trajectory Generation for the N-Trailer Problem Using Goursat Normal Form. IEEE Transactions on Automatic Control, Vol. 40. NO. 5. 1995.

[4] Sklyarenko, Y.; Schreiber, F. and Schumacher W. Maneuvering assistant for truck and trailer combinations with arbitrary trailer hitching. Institute of Control Engineering. Technische Universität Braunschweig. Braunschweig, Germany.

[5] Abdelrahman, M. A contribution to the development of a special-purpose vehicle for handicapped persons. Department of technical mechanics. Technische Universität Ilmenau. Ilmenau, Germany 2014.

[6] Martynenko, Y. Motion control of mobile wheeled robots. Journal of Mathematical Sciences, Vol. 147, No. 2, 2007.

[7] Han, K.; Choi, O.; Kim, J.; Kim, H. and Lee, J. Design and Control of Mobile Robot with Mecanum Wheel. Department of Electrical Engineering, Pohang University of Science and Technology, Pohang, Korea 2009.

[8] Dickerson, S. and Lapin, B. Control of an Onmi-Directional Robotic Vehicle with Mecanum Wheels. Georgia Institute of Technology. Atlanta, United States of America 1991.

[9] Tlale, N. On distributed mechatronics controller for omni-directional autonomous guided vehicles. Department of Industrial and Systems Engineering, University of Pretoria, Pretoria, South Africa 2006.

[10] Mohd, J.; Rizon, M.; Yaacob, S.; Adom A. and Mamat, M. Designing Omni-Directional Mobile Robot with Mecanum Wheel. American Journal of Applied Sciences 3 (5) 2006.

[11] Doroftei, I.; Grosu, V. and Spinu, V. Design and Control of an Omni-Directional Mobile Robot. “Gh. Asachi” Technical University of Iasi, Romania 2008.

[12] Wakchaure, K.; Bhaskar, S.; Thakur, A. and Modak, G. Kinematics Modelling of Mecanum Wheeled Mobile Platform. Department of Mechanical Engineering, S.R.E.S’s College of Engineering, Kopargaon. Department of Mechanical Engineering, P.V.G’s College of Engineering and Technology, Pune.

[13] Matsinos, E. Modelling of the motion of a Mecanum-wheeled vehicle. Institute of Mechatronic Systems, Zurich University of Applied Sciences. Winterthur, Switzerland.

[14] Diegel, O.; Badve, A.; Bright, G.; Potgieter, J. and Tlale, S. Improved Mecanum Wheel Design for Omni-directional Robots. Institute of technology and Engineering, Massey University. Auckland, New Zealand 2002.

[15] Tlale, N. and de Villiers, M. Kinematics and Dynamics Modelling of a Mecanum Wheeled Mobile Platform. 15th International conference on Mechatronics and Machine Vision in Practice. Auckland, New Zealand 2008.

[16] Zimmermann, K.; Zeidis, I. and Behn, C. Mechanics of Terrestrial Locomotion. Springer, 2009.

[17] Zimmermann, K.; Zeidis, I. and Abdelrahman, M. Dynamics of mechanical systems with Mecanum Wheels. DSTA 2014, Lodz, 1.-5.12.2013.

[18] Murray, R. and Sastry, S. Nonholonomic Motion Planning: Steering Using Sinusoids. IEEE Transactions on Automatic Control, Vol. 38, NO. 5, 1993.

[19] Altafini C.; Speranzon, A. and Johansson, K. Hybrid Control of a Truck and Trailer Vehicle. Hybrid Systems: Computation and Control. Springer, 2002.

[20] Kang, J.; Kim, B. and Chung, M. Development of Omni-directional Mobile Robots with Mecanum Wheels Assisting the Disabled in a Factory Environment. International Conference of Control, Automation and Systems 2008.

[21] Xu, P. Mechatronics Design of a Mecanum Wheeled Mobile Robot. Cutting Edge Robotics. Pro literatur Verlag. 2005.

[22] Muir, P. and Neuman, C. Kinematic Modelling of Wheeled Mobile Robots. Carnegie-Mellon University. Pittsburgh, Pennsylvania 1986.

[23] Seegmiller, N. and Kelly, A. Enhanced 3D Kinematic Modeling of Wheeled Mobile Robots. Robotics Institute, Carnegie Mellon University.

[24] Holmberg, R. and Khatib, O. Development and Control of a Holonomic Mobile Robot for Mobile Manipulation Tasks. The International Journal of Robotics Research, Vol. 19, No. 11, November 2000.

[25] Koestler, A. and Bräuln, T. Mobile Robot Simulations with Realistic Error Models. 2nd International Conference on Autonomous Robots and Agents. New Zealand 2004.

[26] Ramirez-Serrano, A. and Kuzyk, R. Modified Mecanum Wheels for Traversing Rough Terrains. Sixth International Conference on Autonomic and Autonomous Systems 2010.

[27] Jungmin, K.; Seungbeom, W.; Jaeyong, K.; Joocheol, D.; Sungshin, K. and Sunil, B. Inertial Navigation System for an Automatic Guided Vehicle with Mecanum Wheels. International Journal of Precision Engineering and Manufacturing, Vol. 13, No. 3, 2012.

[28] Yunan, Z.; Shuangshuang, W. and Jian, Z. Research on Motion Characteristic of Omnidirectional Robot based on Mecanum Wheel. International Conference on Digital Manufacturing & Automation 2010.

[29] Park, M.; Chung, W. and Kim, M. Control of a mobile robot with passive multiple trailers. Proceedings of the 2004 IEEE International Conference on Robotics & Automation. 2004.

[30] Zöbel, D. Mathematical modeling of the kinematics of vehicles. Mathematical model of Technical Processes, 2001.

[31] Martínez, J.; Morales, J.; Mandow, A. and García-Cerezo, A. Steering Limitations for a Vehicle Pulling Passive Trailers. IEEE Transactions on Control Systems Technology, Vol. 16, No. 4, 2008.

FINAL ACKNOWLEDGMENT

To Dr. rer. nat. Igor Zeidis, for his help and support with the mathematical models discussed in this study.

To Dipl.-Ing. (FH) Tobias Kästner, for his help and support during the design stage of the trailer.

To Dipl.-Ing. H.- P. Walkling, for the idea of improving omnidirectional wheels.

To Univ.-Prof. Dipl.-Ing. Jorge Rodriguez, for his support not only as thesis supervisor, but also during the entire process of studying in Germany.

To Univ.-Prof. Dr.-Ing. habil. Klaus Zimmermann, for his exceptional support, supervision and advice during my whole stay in Germany, which was invaluable to develop the study here presented.